ELSEVIER

Physica D 143 (2000) 74–108

PHYSICA D

www.elsevier.com/locate/physd

Heteroclinic cycles in rings of coupled cells

Pietro-Luciano Buono [a], Martin Golubitsky [b,*], Antonio Palacios [c]

[a] *Mathematics Institute, University of Warwick, Coventry CV4 7AL, UK*
[b] *Department of Mathematics, University of Houston, Houston, TX 77204-3476, USA*
[c] *Department of Mathematics, San Diego State University, San Diego, CA 92182-7720, USA*

In the memory of John David Crawford

Abstract

Symmetry is used to investigate the existence and stability of heteroclinic cycles involving steady-state and periodic solutions in coupled cell systems with $\mathbf{D}_n$-symmetry. Using the lattice of isotropy subgroups, we study the normal form equations restricted to invariant fixed-point subspaces and prove that it is possible for the normal form equations to have robust, asymptotically stable, heteroclinic cycles connecting periodic solutions with steady states and periodic solutions with periodic solutions. A center manifold reduction from the ring of cells to the normal form equations is then performed. Using this reduction we find parameter values of the cell system where asymptotically stable cycles exist. Simulations of the cycles show trajectories visiting steady states and periodic solutions and reveal interesting spatio-temporal patterns in the dynamics of individual cells. We discuss how these patterns are forced by normal form symmetries.

Keywords: Heteroclinic cycles; Coupled cell systems; Spatio-temporal patterns; Equivariant bifurcation theory; $\mathbf{D}_n$-symmetry

1. Introduction

Coupled systems of differential equations or cells are often used as models of physical systems. For example, they are used by Hadley et al. [15] and Aronson et al. [2] to model arrays of Josephson junctions and by Kopell and Ermentrout [16,17] and Rand et al. [23] to model central pattern generators (CPGs) in biological systems. Recently, Collins and Stewart [4–6] and Golubitsky et al. [12] have shown that many phase relations observed in animal gaits can be modeled by coupled cell systems. In these works the symmetry of the cell network is important in determining the patterns of oscillation that the system can support. See the works of Dionne et al. [7,8], Golubitsky and Stewart [11], and the related work of Lamb and Melbourne [20].

In this paper, we discuss the existence of heteroclinic cycles in coupled cell systems. Such cycles model intermittency and are known to occur robustly and asymptotically stably in systems with symmetry (see [9,10,14]). Armbruster et al. [1] and Melbourne et al. [22] show that heteroclinic cycles can occur stably in systems with $\mathbf{O}(2)$-symmetry and, in previous numerical work [3], we show that these cycles are also found stably in systems

* Corresponding author.
E-mail addresses: buono@maths.warwick.ac.uk (P.-L. Buono), mg@uh.edu (M. Golubitsky), palacios@euler.sdsu.edu (A. Palacios)

0167-2789/00/$ – see front matter
PII: S0167-2789(00)00097-X

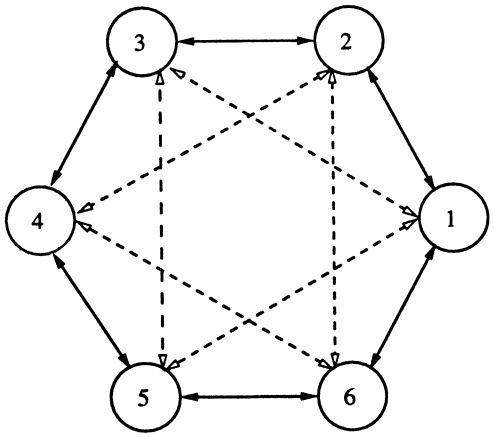

Fig. 1. $\mathbf{D}_6$-symmetric six-cell network with nearest and second nearest neighbor coupling.

with $\mathbf{D}_n$-symmetry, $n \geq 5$. In this paper, we provide the proofs behind the results in [3], continue our studies by showing that heteroclinic cycles also occur in rings of coupled cells (which have structure in addition to $\mathbf{D}_n$-symmetry), and discuss how symmetry forces certain spatio-temporal patterns in the periodic solutions in the cycle.

1.1. Coupled cell systems

We assume that the n cells are identical and that the internal dynamics of each cell is governed by a system of differential equations (that may depend on parameters, which we suppress). That is, for $1 \leq i \leq n$,

$$\frac{\mathrm{d}X_i}{\mathrm{d}t} = f(X_i), \tag{1}$$

where $X_i = (x_{i1}, \ldots, x_{ik}) \in \mathbf{R}^k$ denotes the state variables of cell i and f is smooth and independent of i (since the cells are assumed to be identical). For instance, in biological applications (1) might be a Hodgkin–Huxley type model.

A network is a collection of identical interconnected cells. For example, Fig. 1 illustrates a six-cell network with nearest and next nearest neighbor coupling. We model the interconnected network by a system of differential equations of the form

$$\frac{\mathrm{d}X_i}{\mathrm{d}t} = f(X_i) + \sum_{j \to i} \alpha_{ij} h(X_i, X_j), \tag{2}$$

where h is the coupling function between two cells, the summation is taken over those cells j that are coupled to cell i, and α_{ij} is a matrix of coupling strengths.

1.2. Heteroclinic cycles

A *heteroclinic cycle* is a collection of solution trajectories that connects sequences of equilibria and/or periodic solutions. For a more precise description of heteroclinic cycles and their stability, see the papers of Melbourne et al. [22], Krupa and Melbourne [19], the monograph by Field [10], and the survey paper by Krupa [18].

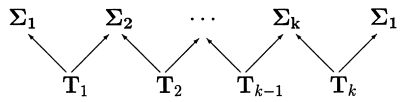

Fig. 2. Pattern inside lattice of subgroups that suggests the existence of heteroclinic cycles.

Melbourne et al. [22] describe a method for finding heteroclinic cycles in symmetric systems of differential equations. Let $\Gamma \subset \mathbf{O}(N)$ be a Lie subgroup and let $g : \mathbf{R}^N \to \mathbf{R}^N$ be Γ-equivariant, i.e.

$$g(\gamma X) = \gamma g(X)$$

for all $\gamma \in \Gamma$. Consider the system

$$\frac{\mathrm{d}X}{\mathrm{d}t} = g(X). \tag{3}$$

Note that $N = kn$ in an n cell system with k state variables in each cell. Equivariance of g implies that whenever $X(t)$ is a solution, so is $\gamma X(t)$. Using fixed-point subspaces, Melbourne et al. [22] suggest a method for constructing heteroclinic cycles connecting equilibria. Suppose that $\Sigma \subset \Gamma$ is a subgroup. Then the fixed-point subspace

$$\mathrm{Fix}(\Sigma) = \{X \in \mathbf{R}^N : \sigma X = X \quad \forall \sigma \in \Sigma\}$$

is a flow invariant subspace [13]. The idea in [22] is to find a sequence of maximal subgroups $\Sigma_j \subset \Gamma$ such that $\dim \mathrm{Fix}(\Sigma_j) = 1$ and submaximal subgroups $T_j \subset \Sigma_j \cap \Sigma_{j+1}$ such that $\dim \mathrm{Fix}(T_j) = 2$ as is shown schematically in Fig. 2. Such configurations of subgroups have the possibility of leading to heteroclinic cycles if saddle–sink connections between equilibria in $\mathrm{Fix}(\Sigma_j)$ and $\mathrm{Fix}(\Sigma_{j+1})$ exist in $\mathrm{Fix}(T_j)$. Since saddle–sink connections are robust in a plane, these heteroclinic cycles are stable to perturbations of g so long as Γ-equivariance is preserved by the perturbation.

1.2.1. Cycles involving periodic solutions and broken symmetry

Near points of Hopf bifurcation, this method for constructing heteroclinic connections can be generalized to include time periodic solutions as well as equilibria. Melbourne et al. [22] do this by augmenting the symmetry group of the differential equations with $\mathbf{S}^1$ — the symmetry group of Poincaré–Birkhoff normal form at points of Hopf bifurcation — and using phase–amplitude equations in the analysis. In these cases the heteroclinic cycle exists only in the normal form equations since some of the invariant fixed-point subspaces disappear when symmetry is broken. However, when that cycle is asymptotically stable, then the cycling-like behavior remains even when the equations are not in normal form. This is proved by using asymptotic stability to construct a flow invariant neighborhood about the cycle and then invoking normal hyperbolicity to preserve the flow invariant neighborhood when normal symmetry is broken. Indeed, as is shown by Melbourne [21], normal form symmetry can be used to produce stable cycling behavior even in systems without any spatial symmetry. More generally, it also follows that if an asymptotically stable cycle can be produced in a truncated normal form equation (say truncated at third- or fifth-order), then cycling-like behavior persists in equations with higher-order terms — even when those terms break symmetry — and the cycling-like behavior is robust.

1.2.2. A cycle with $\mathbf{O}(2)$*-symmetry*

Melbourne et al. [22] prove the existence of robust, asymptotically stable heteroclinic cycles involving time periodic solutions in steady-state/Hopf and Hopf/Hopf mode interactions in systems with $\mathbf{O}(2)$-symmetry. In these symmetry-breaking bifurcations each critical eigenvalue is doubled by symmetry — so the center manifold for a

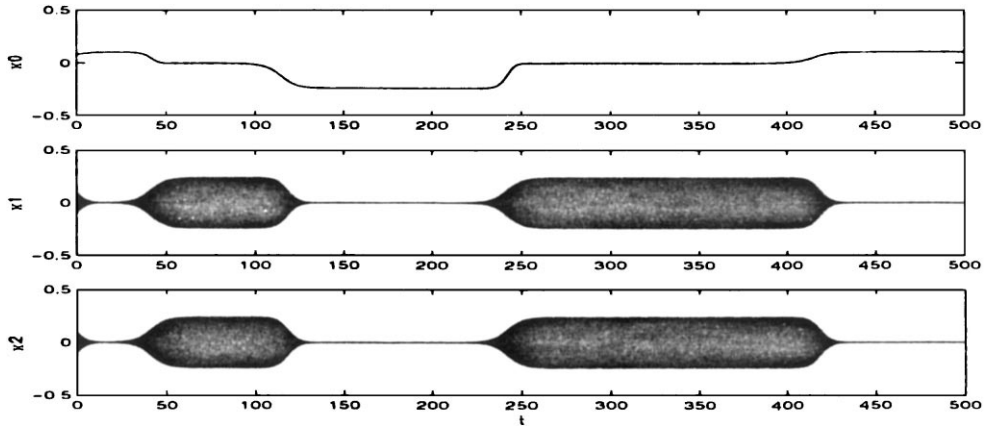

Fig. 3. Cycle connecting a steady-state with a standing wave in a system with $\mathbf{O}(2) \times \mathbf{S}^1$-symmetry with $\mathbf{S}^1$-symmetry due to normal form.

steady-state/Hopf mode interaction is six-dimensional and for a Hopf/Hopf mode interaction it is eight-dimensional. It is well known that $\mathbf{O}(2)$-symmetry-breaking Hopf bifurcations at invariant equilibria lead to two types of periodic solutions: *standing waves* (solutions invariant under a single reflection for all time) and *rotating waves* (solutions whose time evolution is the same as spatial rotation) [13]. Fig. 3 shows a cycle connecting a steady-state with a standing wave obtained from a steady-state/Hopf mode interaction. The time series in this figure are taken from three different coordinates: x_0 is a coordinate in the steady-state mode and $x_1,\ x_2$ are coordinates in the Hopf mode. In these coordinates a standing wave is an oscillation where both coordinates oscillate equally (with just a phase shift). Other types of $\mathbf{O}(2)$ cycles involving only periodic solutions are obtained from Hopf/Hopf mode interactions and examples are shown in [3]. These cycles connect rotating waves with rotating waves and standing waves with standing waves (see also Figs. 11 and 13).

1.2.3. A cycle with $\mathbf{D}_6$-symmetry

In this paper, we prove the existence of heteroclinic cycles involving steady-state and time periodic solutions in differential equations with $\mathbf{D}_n$-symmetry. In [3], we presented numerical evidence for the existence of these cycles. We approach the existence of heteroclinic cycles by studying various mode interactions — in particular, the six-dimensional steady-state/Hopf mode interaction where $\mathbf{D}_n$ acts by its standard representation on the critical eigenspaces. The exact cycles we discuss are found in the normal form equations which have $\mathbf{D}_n \times \mathbf{S}^1$-symmetry when $n = 6$ and $n = 5$ — though much of this discussion is relevant for the general $\mathbf{D}_n$ system.

Reflectional symmetries of a hexagon come in two (nonconjugate) types: those whose line of reflection connects opposite vertices of the hexagon (κ) and those whose line of symmetry connects midpoints of opposite sides ($\gamma\kappa$) [13]. It is known that $\mathbf{D}_6$-symmetry-breaking steady-state bifurcations produce two nontrivial equilibria — one with each type of reflectional symmetry — and $\mathbf{D}_6$-symmetry-breaking Hopf bifurcations produce two standing waves — one with each type of reflectional symmetry. In normal form the symmetry groups of these four solutions are $\mathbf{Z}_2(\kappa) \times \mathbf{S}^1$, $\mathbf{Z}_2(\gamma\kappa) \times \mathbf{S}^1$, $\mathbf{Z}_2(\kappa) \times \mathbf{Z}_2^c$, and $\mathbf{Z}_2(\gamma\kappa) \times \mathbf{Z}_2^c$, where $\mathbf{Z}_2^c = \mathbf{Z}_2(\pi, \pi)$. In Section 2, we show that the lattice of subgroups of $\mathbf{D}_6 \times \mathbf{S}^1$ includes those subgroups pictured in Fig. 4.

Using the ideas in [22], Fig. 4 suggests that robust, asymptotically stable heteroclinic cycles can appear in unfoldings of $\mathbf{D}_6$ normal form symmetry-breaking steady-state/Hopf mode interactions. The cycle connects the first steady-state with the first standing wave with the second steady-state with the second standing wave and back to the first steady-state. We prove that these cycles do exist and present the results of simulation of one such example in Fig. 5.

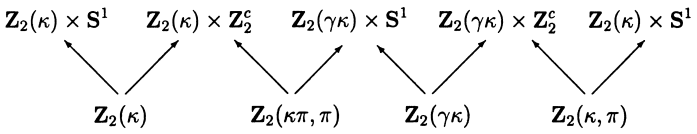

Fig. 4. Subgroups in $\mathbf{D}_6\times\mathbf{S}^1$ lattice that permit existence of heteroclinic cycles.

1.2.4. A cycle in a ring of six coupled cells

A main point of this paper is to demonstrate the existence of robust, asymptotically stable, heteroclinic cycles in rings of coupled cells with $\mathbf{D}_n$-symmetry. Finding such a heteroclinic cycle directly from (2) requires the analysis of a system of differential equations of dimension nk. This task is complicated when either the number of cells n or the number of state variables of each cell k is large. We proceed by using a (Maple-assisted) center manifold reduction to normal form equations on a six-dimensional center manifold. Using this reduction we find parameter values of the cell system where asymptotically stable heteroclinic cycles exist. In order to arrange for the steady-state/Hopf mode interaction to occur, we need to use three state variables per cell.

We verify the results of theory by simulating the coupled cell equations with $n=6$ cells and $k=3$ state variables per cell. This simulation is of an $N=18$ dimensional system of differential equations (see Fig. 6). As noted in [13], the normal form symmetries appear in the coupled cell system as spatio-temporal symmetries where the spatial symmetries are permutations of the cells. These symmetries have the curious property that in one of the standing waves two of the cells are forced to oscillate at twice the frequency of the other four cells [13] (see Fig. 7).

1.2.5. Cycles in $\mathbf{D}_n$-symmetric Hopf/Hopf mode interactions

Numerical simulations show evidence of two types of heteroclinic cycles in $\mathbf{D}_5$-symmetric Hopf/Hopf mode interactions [3]. One cycle connects standing waves and the other connects rotating waves. In Section 4, we prove the existence of the two types of cycles mentioned above in $\mathbf{D}_n$-symmetric Hopf/Hopf mode interactions, $n\geq 5$. The proof of existence is done by inspection of the isotropy lattice of the action of $\mathbf{D}_n\times\mathbf{T}^2$ on $\mathbf{C}^4$, and by studying the normal form equations with respect to this action, to show the existence of appropriate connecting trajectories.

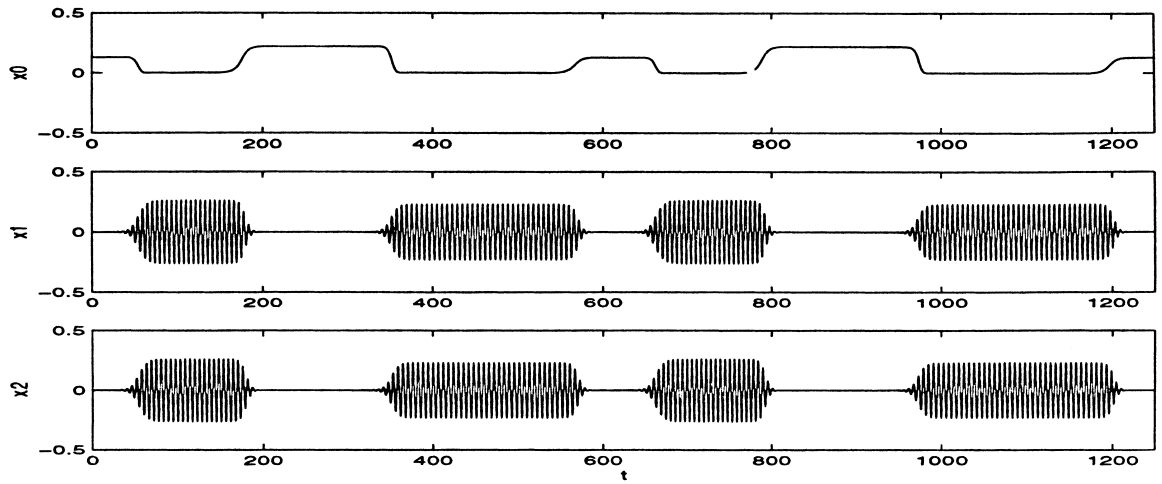

Fig. 5. Heteroclinic cycle connecting steady states $\mathbf{Z}_2(\kappa)\times\mathbf{S}^1$ and $\mathbf{Z}_2(\gamma\kappa)\times\mathbf{S}^1$ with standing waves $\mathbf{Z}_2(\kappa)\times\mathbf{Z}_2^c$ and $\mathbf{Z}_2(\gamma\kappa)\times\mathbf{Z}_2^c$ in a system with $\mathbf{D}_6\times\mathbf{S}^1$-symmetry. Standing waves have different amplitudes. Coefficients listed in (18).

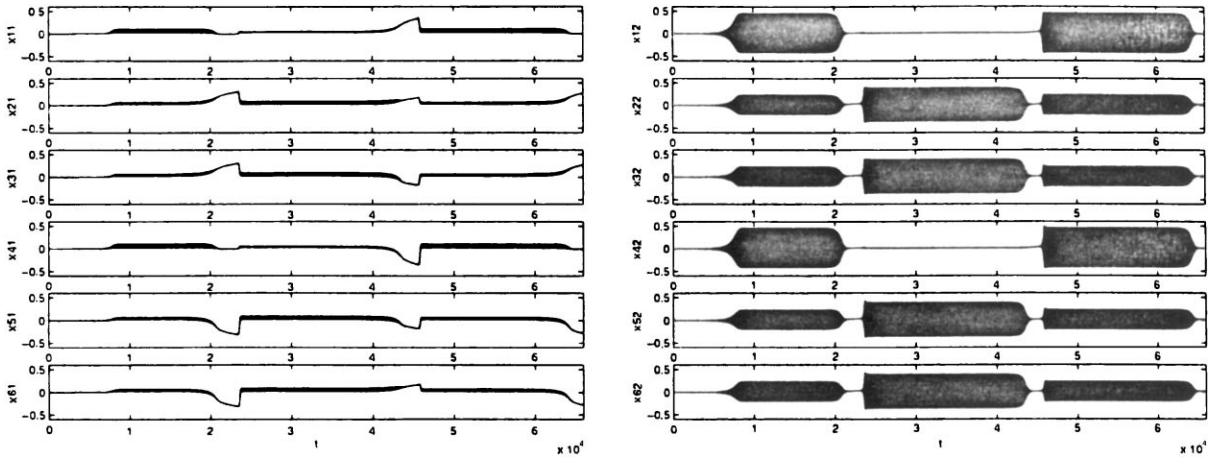

Fig. 6. Heteroclinic cycle in a six-cell ring. Up to third-order, the center manifold flow for this coupled cell system (after scaling) is the same as the flow in Fig. 5: (left) first component and (right) second component of each cell. Coefficients are found in (24).

As explained in Section 4, these cycles are visualized in a $\mathbf{D}_5$-symmetric cell system without computing the reduced equations on the center manifold (see Figs. 11,13 and 14).

This paper is organized as follows. In Section 2, we describe mode interactions in two-parameter families of $\mathbf{D}_6$-equivariant vector fields and prove the existence of robust, asymptotically stable cycles in the normal form equations of steady-state/Hopf mode interactions. We prove the existence of a heteroclinic cycle in a ring of six cells in Section 3. In particular, we show that networks of six identical cells with nearest neighbor and second nearest neighbor coupling can possess these heteroclinic cycles. In Section 4, we study Hopf/Hopf mode interactions in systems with $\mathbf{D}_n$-symmetry ($n \geq 5$) and visualize the cycles in a $\mathbf{D}_5$-symmetric ring of cells. In Section 5, we discuss briefly heteroclinic cycles in other ring systems with $\mathbf{D}_n$-symmetry.

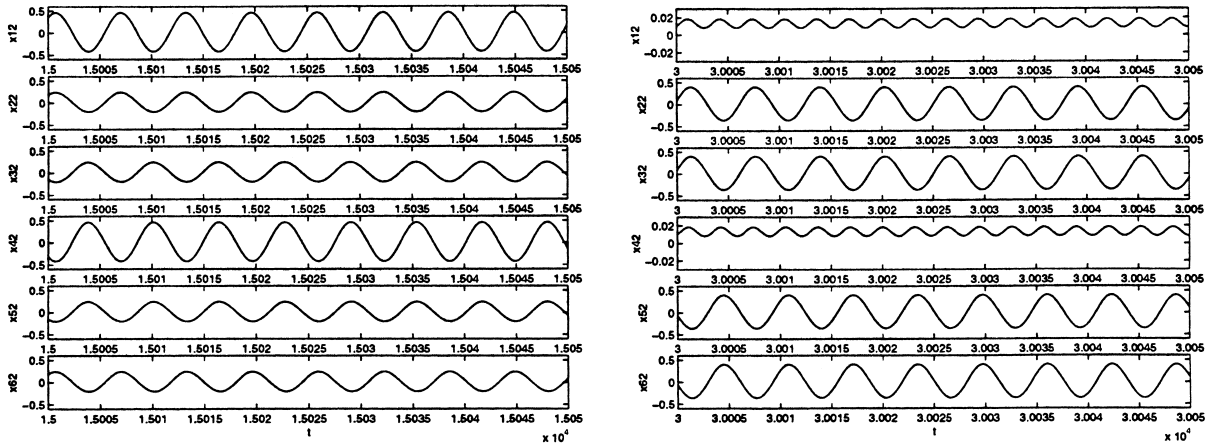

Fig. 7. Enlargement of Fig. 6 illustrating the symmetries of SW1 (left) and SW2 (right) in a cell system. Observe that cells 1 and 4 oscillate at twice the frequency of the other cells in SW2.

2. Mode interactions with $\mathbf{D}_n$-symmetry

Consider the two-parameter $\mathbf{D}_n$-equivariant system of differential equations

$$\frac{\mathrm{d}x}{\mathrm{d}t} = F(x, \lambda, \mu), \tag{4}$$

where $x \in \mathbf{R}^N$ and $\lambda, \mu \in \mathbf{R}$. Assume $x = 0$ is a $\mathbf{D}_n$-symmetric trivial equilibrium, i.e.

$$F(0, \lambda, \mu) = 0.$$

Assume also that the Jacobian $(\mathrm{d}_x F)_{0,0,0}$ has two nonconjugate critical eigenvalues lying on the imaginary axis. Under these assumptions, $(\lambda, \mu) = (0, 0)$ is a *codimension-two* point. The codimension-two point is of one of the following types:

Eigenvalue type	Mode type
$0, 0$	Steady-state/steady-state
$0, \pm\omega\mathrm{i}$	Steady-state/Hopf
$\pm\omega_1\mathrm{i}, \pm\omega_2\mathrm{i}$ (ω_1, ω_2 incommensurate)	Nonresonant Hopf/Hopf

Mode interactions can be specified further by the action of $\mathbf{D}_n$ on the critical eigenspaces. In this paper, we assume that each critical eigenvalue is double and that $\mathbf{D}_n$ acts by its standard two-dimensional action on each critical eigenspace. Moreover, in our analyses we consider only heteroclinic cycles whose nodes include periodic solutions; therefore, we study only the steady-state/Hopf and Hopf/Hopf mode interactions.

In this section, we consider steady-state/Hopf mode interactions. After performing a center manifold reduction on (4), we arrive at a truncated reduced system of ODEs

$$\frac{\mathrm{d}z}{\mathrm{d}t} = g(z, \lambda, \mu), \tag{5}$$

where $z \in \mathbf{C}^3$ and $g(0, \lambda, \mu) = 0$. The eigenvalues of $(\mathrm{d}_z g)_{0,0,0}$ are the critical eigenvalues of $(\mathrm{d}_x F)_{0,0,0}$ on the imaginary axis. By an appropriate change of coordinates we can also assume that (5) is in Poincaré–Birkhoff normal form up to any finite order. This introduces an extra $\mathbf{S}^1$-symmetry, so that g is now $\mathbf{D}_n \times \mathbf{S}^1$-equivariant. We can then choose coordinates $z = (z_0, z_1, z_2)$ such that the $\mathbf{D}_n \times \mathbf{S}^1$-action on $\mathbf{C}^3$ takes the following form [13]. Let $\gamma = 2\pi/n \in \mathbf{Z}_n$ and $\theta \in \mathbf{S}^1 = [0, 2\pi)$, and let κ be a fixed element in $\mathbf{D}_n \sim \mathbf{Z}_n$. Then

$$\begin{aligned} &\gamma(z_0, z_1, z_2) = (\mathrm{e}^{\gamma\mathrm{i}} z_0, \mathrm{e}^{\gamma\mathrm{i}} z_1, \mathrm{e}^{-\gamma\mathrm{i}} z_2), \qquad \kappa(z_0, z_1, z_2) = (\bar{z}_0, z_2, z_1), \\ &\theta(z_0, z_1, z_2) = (z_0, \mathrm{e}^{\theta\mathrm{i}} z_1, \mathrm{e}^{\theta\mathrm{i}} z_2). \end{aligned} \tag{6}$$

As noted in Section 1, robust cycling-like behavior is proved by finding asymptotically stable heteroclinic cycles in a truncated normal form equation.

2.1. The $\mathbf{D}_6 \times \mathbf{S}^1$ lattice of isotropy subgroups

Using these subgroups of $\mathbf{D}_6 \times \mathbf{S}^1$,

$$\begin{aligned} &\mathbf{Z}_2(\kappa) = \{1, \kappa\}, \qquad \mathbf{Z}_2(\gamma\kappa) = \{1, \gamma\kappa\}, \qquad \mathbf{Z}_2^{\mathrm{c}} = \{1, (\pi, \pi)\}, \\ &\mathbf{Z}_2(\kappa, \pi) = \{1, (\kappa\pi)\}, \qquad \mathbf{Z}_2(\kappa\pi, \pi) = \{1, (\kappa\pi, \pi)\}, \qquad \tilde{\mathbf{Z}}_6 = \{(\theta, -\theta) : \theta \in \mathbf{Z}_6\}, \end{aligned}$$

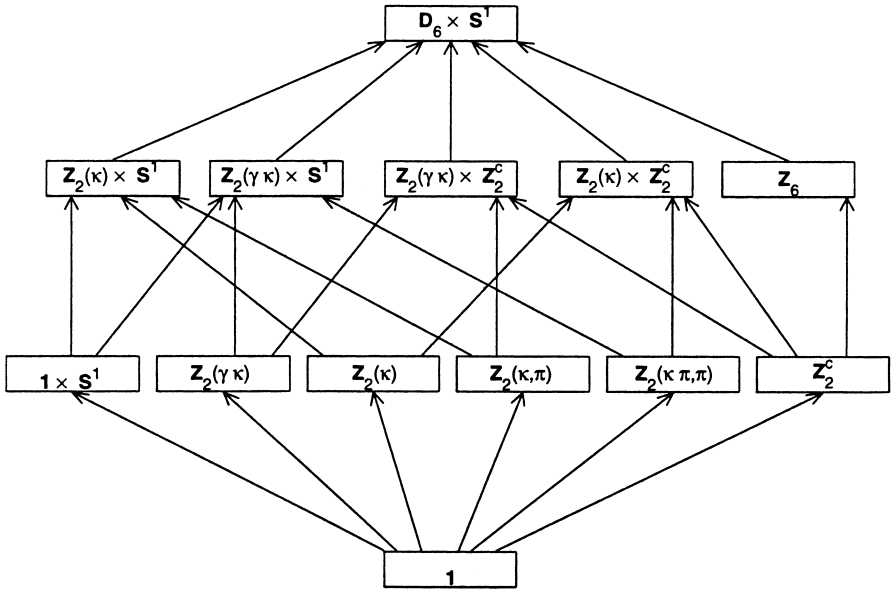

Fig. 8. Lattice of isotropy subgroups of $\mathbf{D}_6 \times \mathbf{S}^1$ acting on $\mathbf{C}^3$, up to conjugacy.

we can determine the lattice of isotropy subgroups of $\mathbf{D}_6 \times \mathbf{S}^1$ as shown in Fig. 8. Embedded in this lattice is Fig. 4 which suggests the possible existence of a heteroclinic cycle in a $\mathbf{D}_6$ system. This cycle would connect equilibrium E_1 ($\mathbf{Z}_2(\kappa) \times \mathbf{S}^1$) to standing wave SW1 ($\mathbf{Z}_2(\kappa) \times \mathbf{Z}_2^c$) to equilibrium E_2 ($\mathbf{Z}_2(\gamma\kappa) \times \mathbf{S}^1$) to standing wave SW2 ($\mathbf{Z}_2(\gamma\kappa) \times \mathbf{Z}_2^c$) and back to E_1. A cycle with a trajectory traveling in the opposite direction is also possible.

To determine whether a cycle actually exists, we need to determine the $\mathbf{D}_6$-invariant functions and $\mathbf{D}_6$-equivariant mappings. Then we use these mappings for calculating branching equations of solutions with maximal isotropy subgroups. Finally, we determine the existence of the cycles and their stability.

2.2. $\mathbf{D}_6$-invariants and $\mathbf{D}_6$-equivariants

Proposition 2.1. *Every real-valued* $\mathbf{D}_6 \times \mathbf{S}^1$-invariant germ is a function of

$$\rho, \quad N, \quad \operatorname{Re} A, \quad \operatorname{Re} B, \quad \operatorname{Re} C, \quad \operatorname{Re} D, \quad \operatorname{Re} E,$$
$$\Delta, \quad \delta \operatorname{Im} A, \quad \delta \operatorname{Im} B, \quad \delta \operatorname{Im} C, \quad \delta \operatorname{Im} D, \quad \delta \operatorname{Im} E,$$

where $\delta = |z_2|^2 - |z_1|^2$ *and*

$$\rho = |z_0|^2, \quad N = |z_1|^2 + |z_2|^2, \quad \Delta = \delta^2, \quad A = z_0^2 \bar{z}_1 z_2,$$
$$B = z_0^6, \quad C = (z_1 \bar{z}_2)^3, \quad D = z_0^2 (z_1 \bar{z}_2)^2, \quad E = z_0^4 z_1 \bar{z}_2.$$

See Appendix A for a proof of this proposition.

Proposition 2.2. *The* $\mathbf{D}_6 \times \mathbf{S}^1$*-equivariant germs* $f : \mathbf{C}^3 \to \mathbf{C}^3$ *are generated over the* $\mathbf{D}^6 \times \mathbf{S}^1$*-invariants by the following mappings*:

$$
\begin{array}{llll}
V^1 = (z_0, 0, 0) & \mathrm{i}\delta V^1, & V^2 = (\bar{z}_0 z_1 \bar{z}_2, 0, 0) & \mathrm{i}\delta V^2,\\
V^3 = (\bar{z}_0^5, 0, 0) & \mathrm{i}\delta V^3, & V^4 = (\bar{z}_0 (\bar{z}_1 z_2)^2, 0, 0) & \mathrm{i}\delta V^4,\\
V^5 = (\bar{z}_0^3 (\bar{z}_1 z_2), 0, 0) & \mathrm{i}\delta V^5, & V^6 = (z_0 (z_1 \bar{z}_2)^3, 0, 0) & \mathrm{i}\delta V^6,\\
V^7 = (0, z_1, z_2) & \mathrm{i}V^7, & \delta V^8 = \delta(0, z_1, -z_2) & \mathrm{i}\delta V^8,\\
V^9 = (0, z_0^2 z_2 \bar{z}_0^2 z_1) & \mathrm{i}V^9, & \delta V^{10} = \delta(0, z_0^2 z_2, -\bar{z}_0^2 z_1) & \mathrm{i}\delta V^{10},\\
V^{11} = (0, \bar{z}_0^4 z_2, z_0^4 z_1) & \mathrm{i}V^{11}, & \delta V^{12} = \delta(0, \bar{z}_0^4 z_2, -z_0^4 z_1) & \mathrm{i}\delta V^{12},\\
V^{13} = (0, \bar{z}_0^2 \bar{z}_1 z_2^2, z_0^2 z_1^2 \bar{z}_2) & \mathrm{i}V^{13}, & \delta V^{14} = \delta(0, \bar{z}_0^2 \bar{z}_1 z_2^2, -z_0^2 z_1^2 \bar{z}_2) & \mathrm{i}\delta V^{14},\\
V^{15} = (0, (\bar{z}_1 z_2)^2 z_2, (z_1 \bar{z}_2)^2 z_1) & \mathrm{i}V^{15}, & \delta V^{16} = \delta(0, (\bar{z}_1 z_2)^2 z_2, -(z_1 \bar{z}_2)^2 z_1) & \mathrm{i}\delta V^{16}.
\end{array}
$$

See Appendix A for a proof of this proposition.

2.3. Branching equations

It follows from Propositions 2.1 and 2.2 that the general $\mathbf{D}_6 \times \mathbf{S}^1$-equivariant mapping has the form $g(z, \lambda, \mu) = (C(z), Q(z)) \in \mathbf{C} \times \mathbf{C}^2$, where

$$
C(z) = C^1 z_0 + C^3 \bar{z}_0 z_1 \bar{z}_2 + C^5 \bar{z}_0^5 + C^7 \bar{z}_0 (\bar{z}_1 z_2)^2 + C^9 \bar{z}_0^3 \bar{z}_1 z_2 + C^{11} z_0 (z_1 \bar{z}_2)^3, \tag{7}
$$

$$
\begin{aligned}
Q(z) = {} & Q^1 \begin{bmatrix} z_1 \\ z_2 \end{bmatrix} + Q^2 \delta \begin{bmatrix} z_1 \\ -z_2 \end{bmatrix} + Q^3 \begin{bmatrix} z_0^2 z_2 \\ \bar{z}_0^2 z_1 \end{bmatrix} + Q^4 \delta \begin{bmatrix} z_0^2 z_2 \\ -\bar{z}_0^2 z_1 \end{bmatrix} + Q^5 \begin{bmatrix} \bar{z}_0^4 z_2 \\ z_0^4 z_1 \end{bmatrix} + Q^6 \delta \begin{bmatrix} \bar{z}_0^4 z_2 \\ -z_0^4 z_1 \end{bmatrix} \\
& + Q^7 \begin{bmatrix} \bar{z}_0^2 \bar{z}_1 z_2^2 \\ z_0^2 z_1^2 \bar{z}_2 \end{bmatrix} + Q^8 \delta \begin{bmatrix} \bar{z}_0^2 \bar{z}_1 z_2^2 \\ -z_0^2 z_1^2 \bar{z}_2 \end{bmatrix} + Q^9 \begin{bmatrix} (\bar{z}_1 z_2)^2 z_2 \\ (z_1 \bar{z}_2)^2 z_1 \end{bmatrix} + Q^{10} \delta \begin{bmatrix} (\bar{z}_1 z_2)^2 z_2 \\ -(z_1 \bar{z}_2)^2 z_1 \end{bmatrix},
\end{aligned} \tag{8}
$$

where $\delta = |z_2|^2 - |z_1|^2$, $C^j = c^j + \mathrm{i}\delta c^{j+1}$, c^j are real-valued $\mathbf{D}_6 \times \mathbf{S}^1$-invariant functions and $Q^j = p^j + q^j \mathrm{i}$ are complex-valued $\mathbf{D}_6 \times \mathbf{S}^1$-invariant functions depending on two parameters λ and μ.

Additionally, the eigenvalue structure of g leads to $c^1(0) = 0$ and $Q^1(0) = \omega \mathrm{i}$. Solving $g = 0$, we find steady-state and periodic solutions that bifurcate from the trivial solution $x = 0$ at the codimension-two point $(\lambda, \mu) = (0, 0)$. These solutions are listed in Table 1, where all coefficients for the branching equations are evaluated at zero.

Next we determine the stability of the branching solutions. We do this by considering the isotypic decomposition of $\mathbf{C}^3$ into a direct sum of Σ-irreducible subspaces

$$
\mathbf{C}^3 = V_0 \oplus V_1 \oplus \cdots \oplus V_q.
$$

In Table 2, we show the isotypic decomposition by each of the isotropy subgroups of solutions. Other isotropy subgroups are shown as well for later use in this section. Note that $\mathrm{Fix}(\Sigma) = V_0$ for each subgroup Σ. Furthermore, observe that when Σ is a subgroup of a periodic solution, $(\mathbf{D}_6 \times \mathbf{S}^1)/\Sigma$ forces one eigenvalue of dg to be zero. The corresponding null vector is also listed in Table 2. In each case, the stability of solutions with maximal isotropy is determined by $\mathrm{tr}(\mathrm{d}g|V_j)$. We compute the Jacobian $\mathrm{d}g$ in complex coordinates

$$
(\mathrm{d}g)(\zeta) = g_{z_0}\zeta_0 + g_{\bar{z}_0}\bar{\zeta}_0 + g_{z_1}\zeta_1 + g_{\bar{z}_1}\bar{\zeta}_1 + g_{z_2}\zeta_2 + g_{\bar{z}_2}\bar{\zeta}_2,
$$

where $\zeta = (\zeta_0, \zeta_1, \zeta_2)$, $g = (g^0, g^1, g^2)$ and $g_{z_j} = (g^0_{z_j}, g^1_{z_j}, g^2_{z_j})$. The eigenvalues of $\mathrm{d}g$ are also listed in Table 2 up to fifth-order in g.

Table 1
Branches of solutions for $\mathbf{D}_6$ steady-state/Hopf mode interaction

Solution	Isotropy subgroup	Orbit representative	Branching equations
Trivial	$\mathbf{D}_6 \times \mathbf{S}^1$	$(0, 0)$	$z = 0$
Steady state, $A_1 = \mathrm{E}_1$	$\mathbf{Z}_2(\kappa) \times \mathbf{S}^1$	$(x, 0, 0)$	$\lambda = -\left(\frac{c_\rho^1 + c^5 x^2}{c_\lambda^1}\right) x^2$
Steady state, $A_3 = \mathrm{E}_2$	$\mathbf{Z}_2(\gamma\kappa) \times \mathbf{S}^1$	$(\mathrm{e}^{\mathrm{i}\gamma/2}x, 0, 0)$	$\lambda = -\left(\frac{c_\rho^1 - c^5 x^2}{c_\lambda^1}\right) x^2$
Standing wave, $A_2 = \mathrm{SW1}$	$\mathbf{Z}_2(\kappa) \times \mathbf{Z}_2^{\mathrm{c}}$	$(0, r, r)$	$\lambda = -\left(\frac{2p_N^1 + p^9 r^2}{p_\lambda^1}\right) r^2$
Standing wave, $A_4 = \mathrm{SW2}$	$\mathbf{Z}_2(\gamma\kappa) \times \mathbf{Z}_2^{\mathrm{c}}$	$(0, r, \mathrm{e}^{-\mathrm{i}\gamma} r)$	$\lambda = -\left(\frac{2p_N^1 - p^9 r^2}{p_\lambda^1}\right) r^2$
Rotating wave, RW	$\mathbf{Z}_6$	$(0, r, 0)$	$\lambda = -\left(\frac{p_\rho^1 + p_N^1 - p^2}{p_\lambda^1}\right) r^2$

Table 2
Isotypic decomposition by isotropy subgroups of $\mathbf{D}_6 \times \mathbf{S}^1$, where $x \in \mathbf{R}$, $z \in \mathbf{C}$

Isotropy	Isotypic decomposition	Null vectors	Eigenvalues[a]
$\mathbf{D}_6 \times \mathbf{S}^1$	$V_0 = \mathbf{C}^3$		p^1 (4 times): c^1 (twice)
$\mathbf{Z}_2(\kappa) \times \mathbf{S}^1$	$V_0 = (x, 0, 0)$		V_0: $2(c_\rho^1 + 2c^5 x^2)x^2$
	$V_1 = (\mathrm{i}x, 0, 0)$		V_1: $-6c^5 x^4$
	$V_2 = (0, z, z)$		V_2: $p_\lambda^1 \lambda + (p_\rho^1 + p^3)x^2 + p^7 x^4$ (*)
	$V_3 = (0, z, -z)$		V_3: $p_\lambda^1 \lambda + (p_\rho^1 - p^3)x^2 - p^7 x^4$ (*)
$\mathbf{Z}_2(\gamma\kappa) \times \mathbf{S}^1$	$V_0 = (\mathrm{e}^{\mathrm{i}\gamma/2}x, 0, 0)$		V_0: $2(c_\rho^1 - 2c^5 x^2)x^2$
	$V_1 = (\mathrm{e}^{\mathrm{i}\gamma/2}\mathrm{i}x, 0, 0)$		V_1: $6c^5 x^4$
	$V_2 = (0, z, \mathrm{e}^{-\gamma\mathrm{i}} z)$		V_2: $p_\lambda^1 + (p_\rho^1 + p^3)x^2 - p^7 x^4$ (*)
	$V_3 = (0, z, -\mathrm{e}^{-\gamma\mathrm{i}} z)$		V_3: $p_\lambda^1 + (p_\rho^1 - p^3)x^2 + p^7 x^4$ (*)
$\mathbf{Z}_2(\kappa) \times \mathbf{Z}_2^{\mathrm{c}}$	$V_0 = (0, z, z)$	$(0, \mathrm{i}, \mathrm{i})$	V_0: $0,\ 4(p_N^1 + p^9 r^2)r^2$
	$V_1 = (x, 0, 0)$		V_1: $c_\lambda^1 \lambda + (2c_N^1 + c^3)r^2 + c^7 r^4$
	$V_2 = (\mathrm{i}x, 0, 0)$		V_2: $c_\lambda^1 \lambda + (2c_N^1 + c^3)r^2 - c^7 r^4$
	$V_3 = (0, z, -z)$		V_3: $-2(p^2 + 2p^9 r^2)r^2$ (*)
$\mathbf{Z}_2(\gamma\kappa) \times \mathbf{Z}_2^{\mathrm{c}}$	$V_0 = (0, z, \mathrm{e}^{-\gamma\mathrm{i}} z)$	$(0, \mathrm{i}, \mathrm{e}^{-\gamma\mathrm{i}}\mathrm{i})$	V_0: $0,\ 4(p_N^1 - p^9 r^2)r^2$
	$V_1 = (\mathrm{e}^{\mathrm{i}\gamma/2}x, 0, 0)$		V_1: $c_\lambda^1 \lambda + (2c_N^1 + c^3)r^2 - c^7 r^4$
	$V_2 = (\mathrm{e}^{\mathrm{i}\gamma/2}\mathrm{i}x, 0, 0)$		V_2: $c_\lambda^1 \lambda + (2c_N^1 + c^3)r^2 + c^7 r^4$
	$V_3 = (0, z, -\mathrm{e}^{-\gamma\mathrm{i}} z)$		V_3: $-2(p^2 - 2p^9 r^2)r^2$ (*)
$\mathbf{Z}_6$	$V_0 = (0, z, 0)$	$(0, \mathrm{i}, 0)$	V_0: $0,\ 2(p_N^1 - p^2 + (2p_\Delta^1 - p_N^2)r^2)r^2$
	$V_1 = (z, 0, 0)$		V_1: c^1 (*)
	$V_2 = (0, 0, z)$		V_2: $2p^2 r^2$ (*)

[a] (*) indicates real part of a complex conjugate pair.

Table 3
Amplitude equations on $\mathrm{Fix}(\Sigma)$

Isotropy subgroup	Fixed-point subspace	Restricted amplitude equations
$\mathbf{Z}_2(\kappa)\times\mathbf{S}^1$	$(x,0,0)$	$\dot{x}=(c^1+c^5x^4)x$
$\mathbf{Z}_2(\gamma\kappa)\times\mathbf{S}^1$	$(\mathrm{e}^{\mathrm{i}\gamma/2}x,0,0)$	$\dot{x}=(c^1-c^5x^4)x$
$\mathbf{Z}_2(\kappa)\times\mathbf{Z}_2^c$	$(0,z,z)$	$\dot{r}=(p^1+p^9r^4)r$
$\mathbf{Z}_2(\gamma\kappa)\times\mathbf{Z}_2^c$	$(0,z,\mathrm{e}^{-\gamma\mathrm{i}}z)$	$\dot{r}=(p^1-p^9r^4)r$
$\mathbf{Z}_2(\kappa)$	(x,z,z)	$\dot{x}=(c^1+c^3r^2+c^5x^4+c^7r^4+c^9r^2x^2+c^{11}r^6)x,\ \ \dot{r}=(p^1+p^3x^2+p^5x^4+p^7r^2x^2+p^9r^4)r$
$\mathbf{Z}_2(\gamma\kappa)$	$(\mathrm{e}^{\mathrm{i}\gamma/2}x,z,\mathrm{e}^{-\gamma\mathrm{i}}z)$	$\dot{x}=(c^1+c^3r^2-c^5x^4-c^7r^4-c^9r^2x^2-c^{11}r^6)x,\ \ \dot{r}=(p^1+p^3x^2-p^5x^4-p^7r^2x^2-p^9r^4)r$
$\mathbf{Z}_2(\kappa,\pi)$	$(x,z,-z)$	$\dot{x}=(c^1-c^3r^2+c^5x^4+c^7r^4-c^9r^2x^2-c^{11}r^6)x,\ \ \dot{r}=(p^1-p^3x^2-p^5x^4-p^7r^2x^2-p^9r^4)r$
$\mathbf{Z}_2(\kappa\pi,\pi)$	$(\mathrm{i}x,z,-z)$	$\dot{x}=(c^1-c^3r^2-c^5x^4-c^7r^4+c^9r^2x^2+c^{11}r^6)x,\ \ \dot{r}=(p^1-p^3x^2+p^5x^4-p^7r^2x^2+p^9r^4)r$

In Table 3, we list maximal and submaximal isotropy subgroups and their fixed-point subspaces. Since g is in Poincaré–Birkhoff normal form, the restriction of (7) and (8) to each of the fixed-point subspaces decouples into amplitude/phase equations. Thus, using polar coordinates $z_j = r_j\,\mathrm{e}^{\mathrm{i}\theta_j}$, we arrive at the amplitude equations listed in the last column of Table 3. Observe that zeros of the amplitude equations with $r=0$ correspond to steady states of (7), while zeros with $r\neq 0$ correspond to standing waves. Both types of solutions with maximal isotropy have effective dimension equal to 1. Note also that the effective dimension of the fixed-point subspaces of the submaximal subgroups $\mathbf{Z}_2(\kappa)$, $\mathbf{Z}_2(\gamma\kappa)$, $\mathbf{Z}_2(\kappa)$, and $\mathbf{Z}_2(\gamma\kappa)$ is 2. Now let

$$P_0=\mathrm{Fix}(\mathbf{Z}_2(\kappa,\pi)),\qquad P_1=\mathrm{Fix}(\mathbf{Z}_2(\kappa)),\qquad P_2=\mathrm{Fix}(\mathbf{Z}_2(\kappa\pi,\pi)),\qquad P_3=\mathrm{Fix}(\mathbf{Z}_2(\gamma\kappa)).\tag{9}$$

Then these solutions lie on flow-invariant lines $L_j = P_j\cap P_{j-1}$. Next we show that robust heteroclinic cycles exist and determine conditions for their stability.

2.4. Existence and stability of a cycle

We consider here conditions similar to those used by Melbourne et al. [22] for proving the existence of a heteroclinic cycle, except that now we have a system with $\mathbf{D}_6$-symmetry instead of $\mathbf{O}(2)$-symmetry. We assume that $\mu=0$ and view (7) and (8) as a bifurcation problem in λ. Then, we encounter four symmetry-breaking branches of solutions bifurcating simultaneously at $\lambda=0$. Two of the branches contain steady states (not related by symmetry) and two contain standing waves (not related by symmetry). Substitution of solutions of the branching equations in the eigenvalues of $\mathrm{d}g$ leads to the following coefficients at lowest order, which are needed to assert the existence of the cycle.

$$\delta_1=p^1_\rho-c^1_\rho\frac{p^1_\lambda}{c^1_\lambda}+p^3,\qquad \delta_2=p^1_\rho-c^1_\rho\frac{p^1_\lambda}{c^1_\lambda}-p^3,\qquad \delta_3=2c^1_N+c^3-2p^1_N\frac{c^1_\lambda}{p^1_\lambda},$$
$$\delta_4=2c^1_N-c^3-2p^1_N\frac{c^1_\lambda}{p^1_\lambda},\qquad \delta_5=(p^1_\rho+p^3)\frac{c^1_\lambda}{p^1_\lambda c^1_\rho}+(2c^1_N+c^3)\frac{p^1_\lambda}{2p^1_Nc^1_\lambda},$$
$$\delta_6=(p^1_\rho-p^3)\frac{c^1_\lambda}{p^1_\lambda c^1_\rho}+(2c^1_N-c^3)\frac{p^1_\lambda}{2p^1_Nc^1_\lambda}.$$

Table 4
Signs of eigenvalues along primary branches

Equilibrium in	$\mathrm{Fix}(\mathbf{Z}_2(\kappa))$	$\mathrm{Fix}(\mathbf{Z}_2(\kappa\pi,\pi))$	$\mathrm{Fix}(\mathbf{Z}_2(\gamma\kappa))$	$\mathrm{Fix}(\mathbf{Z}_2(\kappa,\pi))$
$\mathrm{Fix}(\mathbf{Z}_2(\kappa)\times\mathbf{S}^1)$	$\mathrm{sgn}(\delta_1)$			$\mathrm{sgn}(\delta_2)$
$\mathrm{Fix}(\mathbf{Z}_2(\kappa)\times\mathbf{Z}_2^c)$	$\mathrm{sgn}(\delta_3)$	$\mathrm{sgn}(\delta_4)$		
$\mathrm{Fix}(\mathbf{Z}_2(\gamma\kappa)\times\mathbf{S}^1)$		$\mathrm{sgn}(\delta_2)$	$\mathrm{sgn}(\delta_1)$	
$\mathrm{Fix}(\mathbf{Z}_2(\gamma\kappa)\times\mathbf{Z}_2^c)$			$\mathrm{sgn}(\delta_3)$	$\mathrm{sgn}(\delta_4)$

Theorem 2.3. *Consider the general* $\mathbf{D}_6\times\mathbf{S}^1$*-equivariant system* (7) and (8) *with* $\mu=0$ *and solutions as listed in Table* 1. *For* $\lambda>0$, *there exists a branch of robust heteroclinic cycles as suggested in Fig.* 4 *if*

$$c_\lambda^1>0,\qquad c_\rho^1<0,\qquad p_\lambda^1>0,\qquad p_N^1<0, \tag{10}$$

$$\mathrm{sgn}(\delta_1)=\mathrm{sgn}(\delta_4)=-\mathrm{sgn}(\delta_2)=-\mathrm{sgn}(\delta_3), \tag{11}$$

$$\delta_5>-2,\qquad \delta_6>-2. \tag{12}$$

Proof. Observe that all primary bifurcations of solutions are of pitchfork type. Conditions (10) imply that the trivial solution is subcritically asymptotically stable, while the nontrivial solutions are supercritical. In order to prove the existence of the cycle shown in Fig. 4, we must show that in each plane P_j three conditions are satisfied.

1. One of the equilibria is a saddle and the other a sink. Specifically, E_1 is a saddle and SW1 a sink in P_1; SW1 is a saddle and E_2 a sink in P_2; E_2 is a saddle and SW2 a sink in P_3; SW2 is a saddle and E_1 a sink in P_4. The cycle can also be constructed in the reverse direction by interchanging saddles and sinks.
2. There are no other equilibria.
3. Solutions are bounded near the origin.

We verify part 1 as follows. Consider the transition $\mathrm{E}_1\overset{P_1}{\to}\mathrm{SW1}$. Assumptions (10) and Table 2 indicate that both solutions, E_1 and SW1, have negative eigenvalues along tangent directions to the corresponding fixed-point subspaces $\mathrm{Fix}(\mathbf{Z}_2(\kappa)\times\mathbf{S}^1)$ and $\mathrm{Fix}(\mathbf{Z}_2(\kappa)\times\mathbf{Z}_2^c)$. Inside P_1, symmetry forces the remaining eigenvectors to be perpendicular to those fixed-point subspaces. A Taylor series expansion of the corresponding eigenvalues leads to coefficients δ_1 and δ_3, which appear in the column for $\mathrm{Fix}(\mathbf{Z}_2(\kappa))$ in Table 4. When δ_1 and δ_3 are nonzero, the sign of the relevant eigenvalues are determined near bifurcation by the sign of δ_j. Similar calculations for the remaining transitions complete the entries in Table 4. When (10) and (11) hold, 1 is verified when $\lambda>0$. We use the following results to verify parts 2 and 3.

Proposition 2.4 (Melbourne et al. [22]). *Consider the system of ODEs*

$$\frac{\mathrm{d}x}{\mathrm{d}t}=(a_1\lambda+b_1x^2+c_1y^2)x,\qquad \frac{\mathrm{d}y}{\mathrm{d}t}=(a_2\lambda+c_2x^2+b_2y^2)y, \tag{13}$$

where $a_1,a_2>0$, *and* $b_1,b_2<0$. *Then all trajectories starting within a circle of radius* $\mathbf{O}(\sqrt{\lambda})$ *stay bounded near the origin if* $\epsilon=(c_1a_2/b_2a_1)+(c_2a_1/b_1a_2)>-2$.

Remark 2.5 (Melbourne et al. [22]). *If the equilibria in* (13) *on the axes are a pair of saddles and a pair of sinks, then there are no equilibria off the axes.*

Part 2. follows by applying Proposition 2.4 and Remark 2.5 to the appropriate amplitude equations that appear in Table 3.

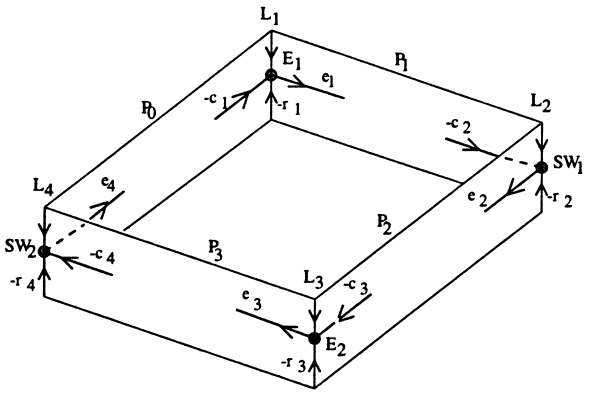

Fig. 9. Contracting and expanding eigenvalues of the heteroclinic cycle shown in Fig. 4.

Finally, we verify part 3. by showing that solutions starting near the origin are bounded in P_1. From the amplitude equations shown in Table 3, we find

$$\dot{x} = (c_\lambda^1\lambda + c_\rho^1 x^2 + (2c_N^1 + c^3)r^2)x, \qquad \dot{r} = (p_\lambda^1\lambda + (p_\rho^1 + p^3)x^2 + 2p_N^1 r^2)r.$$

After applying Proposition 2.4, we arrive at (12). Similar calculations for the remaining invariant planes yield δ_6 in (12). Hence, when $\lambda > 0$, 1–3 show the existence of a heteroclinic cycle. □

Note that the robustness of saddle–sink connections guarantees the existence of the cycle in an open region in parameter space. We now address the stability of the heteroclinic cycle with the aid of Fig. 9. At each equilibria A_j, define the maximum real part of the eigenvalues of $(\mathrm{d}g)_{A_j}$ as follows. The strongest expanding eigenvalue of the equilibrium A_j is e_j, the weakest contracting eigenvalue transverse to $P_{j-1} + P_j$ is t_j, the weakest contracting eigenvalue in the radial direction is r_j, and the weakest contracting eigenvalue restricted to P_{j-1} is c_j (see Table 5). Under these assumptions, r_j, c_j, and e_j are positive, and t_j is negative. In the absence of transverse eigenvalues, set $t_j = -\infty$.

Theorem 2.6 (Melbourne et al. [22]). *Consider a heteroclinic cycle connecting steady states and standing waves as in Theorem* 2.3. *Let $W^{\mathrm{u}}(A_j)$ denote the unstable manifold of the equilibrium A_j. Assume that for each j, there is a flow-invariant subspace P_j such that $W^{\mathrm{u}}(A_j) \subset P_j$ and A_{j+1} is a sink in P_j. Then the heteroclinic cycle is asymptotically stable when*

$$\prod_{j=1}^{k} \min\{c_j, e_j - t_j\} > \prod_{j=1}^{k} e_j. \tag{14}$$

Using (14), we arrive at the following result.

Theorem 2.7. *Assume the following conditions are satisfied*:

$$p^2 > 0, \tag{15}$$

$$|\delta_1\delta_4| < |\delta_2 \min\{-\delta_3, \delta_4 + 2p^2\}|, \tag{16}$$

$$|\delta_2\delta_3| < |\delta_1 \min\{-\delta_4, \delta_3 + 2p^2\}|. \tag{17}$$

Then the heteroclinic cycle of Theorem 2.3 *is asymptotically stable*.

Table 5
Eigenvalues along the cycle

Eigenvalue	Restriction
$-r_j$	L_j
$-c_j$	P_{j-1}
e_j	P_j
t_j	Normal to $P_{j-1}+P_j$

Table 6
Eigenvalues along the cycle

Equilibrium	Contracting c_j	Expanding e_j	Transverse t_j
E_1	$-\delta_2,\ -2c_\rho^1$	δ_1	$-6c^5$
E_2	$-\delta_2,\ 2c_\rho^1$	δ_1	$6c^5$
SW1	$-\delta_3,\ -4p_N^1$	δ_4	$-2p^2(0)$
SW2	$-\delta_3,\ -4p_N^1$	δ_4	$-2p^2(0)$

Proof. The existence of the desired subspaces P_j follows from (10) and (11). Next we verify the structure of the eigenvalues at each equilibrium. When $\delta_1 > 0$, the direction of motion is $A_1 \to A_2 \to A_3 \to A_4$. The opposite direction is obtained when $\delta_1 < 0$. Now assume $\delta_1 > 0$.

From Table 4, we find contracting, expanding, and transverse eigenvalues as in Table 6. Since $\delta_1 > 0$ it follows from (11) that $\delta_4 > 0, \delta_2 < 0$, and $\delta_3 < 0$. These conditions together with (10) imply that all contracting and expanding eigenvalues are positive. From (15), we note that transverse eigenvalues are negative at the standing waves. At the steady states, however, one of the transverse eigenvalues must be positive — either $-6c^5$ or $6c^5$. Since these eigenvalues are determined to fifth-order (see Table 4), they are dominated by the remaining eigenvalues and do not play a role in the stability of the cycle. Theorem 2.6 is still applicable. Substitution of the eigenvalues (to third-order) in (14) yields (16) and (17), while $-2p^2 < 0$ implies (15). When $\delta_1 < 0$, the roles of δ_1 and δ_2 are reversed and the roles of δ_3 and δ_4 are also reversed. Similar calculations yield (17). □

Using the general $\mathbf{D}_6 \times \mathbf{S}^1$-equivariant map (7) and (8), we numerically integrate the system (5) with the following coefficients

$$c^1 = \lambda - 1.5\rho - 4N, \qquad c^2 = 1.3, \qquad c^3 = -9, \qquad c^5 = 0.5,$$
$$p^1 = 1.2\lambda - 3\rho - N, \qquad p^9 = 4, \qquad p^2 = 4, \qquad p^3 = 4, \qquad q^1 = 0.8\lambda + 1, \qquad q^9 = 8, \tag{18}$$

and all other coefficients set to zero. The results are shown in Fig. 5 where $\mathrm{Re}(z_i)$, $i = 1, 2, 3$, is plotted. The two standing waves can be distinguished by their amplitudes.

3. A network of coupled cells with $\mathbf{D}_6$-symmetry

Consider a coupled cell system with nearest neighbor and next nearest neighbor coupling in a ring of six identical cells as in Fig. 1. We show that a heteroclinic cycle between equilibria and standing waves can occur in these coupled cell systems by performing a center manifold reduction to the normal form equations of Section 2 at a steady-state/Hopf mode interaction point. From the reduction we then find parameter values of the cell system where an asymptotically stable cycle exists. We discuss how patterns in the cell dynamics are forced by the symmetries of the normal form equations.

Table 7
Eigenvalues of L

Irreducible representation	Subspace	Eigenvalues of L
Trivial 1D	V_0	J
Standard $\mathbf{D}_6$	$V_1,\ V_5$	$J-A-3B$
Standard $\mathbf{D}_3$	$V_2,\ V_4$	$J-3A-3B$
Nontrivial 1D	V_3	$J-4A$

Let X_i denote cell i. Assuming that each cell is described by k state variables $X_i = (x_{i1}, \dots, x_{ik}) \in \mathbf{R}^k$, we have a system of six equations

$$\frac{\mathrm{d}X_i}{\mathrm{d}t} = F(X_i, \lambda) + A(X_{i+1} - 2X_i + X_{i-1}) + B(X_{i+2} - 2X_i + X_{i-2}), \quad i = 1, \dots, 6, \tag{19}$$

where $F : \mathbf{R}^k \to \mathbf{R}^k$ is an arbitrary smooth function that satisfies $F(0) = 0$, λ a bifurcation parameter, and A and B are $k \times k$ constant matrices which define the strength of the nearest neighbor and next nearest neighbor coupling, respectively. Note that addition in the indices is taken mod 6. The linearization of (19) at the origin is

$$L = \begin{bmatrix} J-2A-2B & A & B & 0 & B & A \\ A & J-2A-2B & A & B & 0 & B \\ B & A & J-2A-2B & A & B & 0 \\ 0 & B & A & J-2A-2B & A & B \\ B & 0 & B & A & J-2A-2B & A \\ A & B & 0 & B & A & J-2A-2B \end{bmatrix},$$

where $J = (\mathrm{d}F)_0$. The eigenvalues of L can be calculated by complexifying $X = (X_1, \dots, X_6) \in \mathbf{R}^{6k}$ to $\mathbf{C}^{6k}$. Let $\zeta = \exp\{\frac{1}{3}\pi \mathrm{i}\}$ be a sixth root of unity in $\mathbf{C}$ and consider the decomposition

$$\mathbf{C}^{6k} = V_0 \oplus \cdots \oplus V_5,$$

where

$$V_j = \{[v, \zeta^j v, \zeta^{2j} v, \zeta^{3j} v, \zeta^{4j} v, \zeta^{5j}] : v \in \mathbf{R}^n\}$$

are invariant subspaces under L. A calculation shows that the eigenvalues of $L|V_j$ are those of $J - 2(A+B) + (\zeta^j + \zeta^{5j})A + (\zeta^{2j} + \zeta^{4j})B$ (see Table 7). Observe that $L|V_0$ and $L|V_3$ have simple eigenvalues, while other subspaces have eigenvalues of multiplicity 2. When $J - A - 3B$ has a zero real eigenvalue and a purely imaginary eigenvalue, each of multiplicity 2, then we have symmetry-breaking steady-state/Hopf mode interactions in (19). This mode interaction occurs in $V_1 \oplus V_5$ which is the standard representation of $\mathbf{D}_6$, and requires that $k \geq 3$. Next we seek conditions for the eigenvalues of the remaining subspaces to have negative real part.

Proposition 3.1. *Assume $k = 3$ in* (19) *and*

$$J = \begin{bmatrix} \alpha & 0 & 0 \\ 0 & \alpha & -\omega \\ 0 & \omega & \alpha \end{bmatrix},$$

where $\alpha < 0$ in the linearization of (19). *Assume diagonal diffusive couplings of the form $A = -aI$ and $B = -bI$, where $a < 0$, $-3b < a < -b$. Then the eigenvalues of $L|V_2$ and $L|V_3$ have negative real parts, and the real parts of the eigenvalues of $L|V_1$ are zero if $\alpha + a + 3b = 0$.*

Proof. Direct calculations show that eigenvalues of $L|V_2$ and $L|V_3$ are those of $J - 3aI - 3bI$ and $J - 4aI$, respectively. Note that eigenvalues of J are α and $\alpha \pm \omega\mathrm{i}$, which have negative real part. Since $a+b < 0$ and $a < 0$, it follows that eigenvalues of $J - 3aI - 3bI$ and $J - 4aI$ also have negative real parts. The eigenvalues of $L|V_1$ are those of $J + aI + 3bI$ with real part $\alpha + a + 3b$. □

3.1. Center manifold reduction

Under the conditions of Proposition 3.1, the flow restricted to the irreducible representation of the standard action of $\mathbf{D}_6$ is asymptotically stable inside $\mathbf{R}^{6k}$. We can then consider a center manifold reduction onto the center subspace $V_1 \oplus V_5$. Before performing the reduction, we must put (19) in a suitable form. Let $X = (x_{11}, \ldots, x_{1k}, \ldots, x_{61}, \ldots, x_{6k})$ and write,

$$\frac{\mathrm{d}X_i}{\mathrm{d}t} = LX + f(X_i, \lambda), \tag{20}$$

where $f(X_i, \lambda) = F(X, \lambda) - LX$ contains only nonlinear terms. The action of $\mathbf{D}_6$ on X is generated by the cyclic permutation $\gamma = (1\,2\,3\,4\,5\,6)$ and the flip $\kappa = (2\,6)(3\,5)$. Let $U = (u_1, \ldots, u_{18})$. We transform the system from X coordinates to U coordinates using the linear transformation $X = PU$, where the columns of P are the eigenvectors of the action of $\mathbf{D}_6$ on $\mathbf{C}^{6k}$. In the new coordinate system, we have

$$\frac{\mathrm{d}U_i}{\mathrm{d}t} = \tilde{L}U_i + \tilde{f}(U, \lambda), \tag{21}$$

where $L = \mathrm{diag}(J - A - 3B,\ J - A - 3B,\ J - 3A - 3B,\ J - 3A - 3B,\ J - 4A,\ J)$ and $\tilde{f} = P^{-1} f(PU)$.

It follows from Proposition 3.1 that the first two columns in $\tilde{L}$ span the center eigenspace, and all other columns span spaces with negative eigenvalues. In the new coordinates U, the action of $\mathbf{D}_6$ on the ring of cells is given by $[\tilde{\gamma}] = P^{-1}[\gamma]P$ and $[\tilde{\kappa}] = P^{-1}[\kappa]P$. Observe that the action of $[\tilde{\gamma}]$ and $[\tilde{\kappa}]$ on the center eigenspace is not yet of the form (6). We must introduce an additional linear change of coordinates. Let $V = (v_1, v_2, \ldots, v_{18})$, $w_0 = v_1 + v_4\mathrm{i}$, $w_1 = v_2 + v_3\mathrm{i}$, $w_2 = v_5 + v_6\mathrm{i}$, and $s_0 = u_1 + u_4\mathrm{i}$, $s_1 = u_2 + u_5\mathrm{i}$, $s_2 = u_3 + u_6\mathrm{i}$. We change coordinates on the center eigenspace as follows:

$$s_0 = w_0, \qquad s_1 = w_1 + \bar{w}_2, \qquad s_2 = (w_1 - \bar{w}_2)\mathrm{i}.$$

In real coordinates, this last change of coordinates is of the form $U = QV$, where

$$Q = \begin{bmatrix} Q_1 & 0 & 0 \\ 0 & I_6 & 0 \\ 0 & 0 & I_6 \end{bmatrix}, \qquad Q_1 = \begin{bmatrix} 1 & 0 & 0 & 0 & 0 & 0 \\ 0 & 1 & 0 & 0 & 1 & 0 \\ 0 & 0 & -1 & 0 & 0 & -1 \\ 0 & 0 & 0 & 1 & 0 & 0 \\ 0 & 0 & 1 & 0 & 0 & -1 \\ 0 & 1 & 0 & 0 & -1 & 0 \end{bmatrix},$$

and I_6 is a 6×6 identity matrix. Under the transformation $U = QV$, (21) becomes

$$\frac{\mathrm{d}V_i}{\mathrm{d}t} = \hat{L}V_i + \hat{f}(V, \lambda), \tag{22}$$

where $\hat{L} = \tilde{L}$, since Q_1 commutes with $J - A - 3B$, and $\hat{f} = Q^{-1}P^{-1}f(PQV)$. Using complex coordinates, it can be shown that the $\mathbf{D}_6$-action on the center eigenspace (w_0, w_1, w_2) is the same as (6). The cell system (22) is now in a suitable form for a center manifold reduction [24].

Table 8
Patterns in solutions forced by isotropy in a six-cell system

Solution	Isotropy subgroup	Pattern of solution
Trivial	$\mathbf{D}_6 \times \mathbf{S}^1$	$X = (0, 0, 0, 0, 0, 0)$
E_1	$\mathbf{Z}_2(\kappa) \times \mathbf{S}^1$	$X = (X_1, X_2, X_3, X_4, X_3, X_2)$
E_2	$\mathbf{Z}_2(\gamma\kappa) \times \mathbf{S}^1$	$X = (X_1, X_1, X_3, X_4, X_4, X_3)$
SW1	$\mathbf{Z}_2(\kappa) \times \mathbf{Z}_2^c$	$X(t) = (X_1(t), X_2(t), X_2(t+\frac{1}{2}T), X_1(t+\frac{1}{2}T), X_2(t+\frac{1}{2}T), X_2(t))$
SW2	$\mathbf{Z}_2(\gamma\kappa) \times \mathbf{Z}_2^c$	$X(t) = (X_1(t), X_1(t), X_3(t), X_1(t+\frac{1}{2}T), X_1(t+\frac{1}{2}T), X_3(t))$, where $X_3(t) = X_3(t+\frac{1}{2}T)$

3.2. Consequences of normal form symmetries

We now interpret how symmetries of periodic solutions in the normal form equations (7) and (8) appear in period T periodic solutions $X(t)$ of (19). Let $X(t) = (X_1(t), \ldots, X_6(t)) \in \mathbf{R}^{6k}$. Spatial symmetries in $\mathbf{D}_6$ act as permutations of the cells while symmetries in $\mathbf{S}^1$ act as phase shift symmetries [13]. The results are listed in Table 8. There are two types of periodic solutions in our cycles: the standing waves SW1 and SW2. We illustrate the restrictions forced by isotropy on SW2.

Standing wave SW2. The periodic solution $X(t)$ has spatial symmetry $\gamma\kappa = (1\,2)(3\,6)(4\,5)$. Therefore,

$$X(t) = (X_1(t), X_1(t), X_3(t), X_4(t), X_4(t), X_3(t)).$$

The $\mathbf{Z}_2^c$ action permutes the cells by $(1\,4)(2\,5)(3\,6)$ and shifts time by half a period. Thus,

$$X(t) = (X_4(t+\tfrac{1}{2}T), X_4(t+\tfrac{1}{2}T), X_3(t+\tfrac{1}{2}T), X_1(t+\tfrac{1}{2}T), X_1(t+\tfrac{1}{2}T), X_3(t+\tfrac{1}{2}T)).$$

Combining the restrictions on $X(t)$ placed by both symmetries yields $X_4(t) = X_1(t+\frac{1}{2}T)$ and $X_3(t) = X_3(t+\frac{1}{2}T)$. Thus, cells 3 and 6 are forced to oscillate at twice the frequency of the other cells. Oscillation in the ring of cells now has the pattern

$$X(t) = (X_1(t), X_1(t), X_3(t), X_1(t+\tfrac{1}{2}T), X_1(t+\tfrac{1}{2}T), X_3(t)),$$

where $X_3(t) = X_3(t+\frac{1}{2}T)$.

3.3. Example

We now perform a (Maple-assisted) center manifold reduction on a cell system of the form (19), with $k = 3$, $a = -2$, $b = 1$, $\alpha = -1$, $\omega = 1$, and

$$F(X_i, \lambda) = \begin{bmatrix} b_{11}\lambda x_{i1} \\ b_{22}\lambda x_{i2} + b_{23}\lambda x_{i3} \\ b_{32}\lambda x_{i2} + b_{33}\lambda x_{i3} \end{bmatrix} + \begin{bmatrix} a_{11}x_{i1}^2 + a_{12}x_{i1}x_{i3} + a_{13}x_{i2}^2 + a_{14}x_{i1}x_{i2}^2 \\ a_{21}x_{i1}^2 + a_{22}x_{i1}x_{i2} + a_{23}x_{i1}x_{i3} + a_{24}x_{i3}^2 + a_{25}x_{i1}^3 \\ a_{31}x_{i1}x_{i2} + a_{32}x_{i3}^2 + a_{33}x_{i1}^2x_{i2} + a_{34}x_{i1}^2x_{i3} + a_{35}x_{i3}^3 \end{bmatrix}. \tag{23}$$

After the reduction is completed, we need to find parameter values for the coefficients of the linear and nonlinear terms in (23) so that the vector field restricted to the center manifold reduces, to third-order, to the general $\mathbf{D}_6 \times \mathbf{S}^1$-equivariant map of Eqs. (7) and (8). Term by term comparison leads to the following relations for the coefficients of the linear terms:

$$\omega = q^1(0), \qquad b_{11} = c_\lambda^1, \qquad \tfrac{1}{2}(b_{22} + b_{33}) = p_\lambda^1, \qquad \tfrac{1}{2}(b_{23} + b_{32}) = q_\lambda^1.$$

The following proposition indicates how to find the coefficients of the nonlinear terms.

Proposition 3.2. *Set $a_{13} = a_{21} = 1$ in* (23). *Let C_X denote the space of coefficients of the remaining nonlinear terms, i.e. $C_X = \{a_{11}, \ldots, a_{35}\}$. Let C_N be the space of coefficients of nonlinear terms in the normal form equations* (7) and (8), *truncated at third-order, i.e. $C_N = \{c_\rho^1, c_N^1, c^2, c^3, p_N^1, q_N^1, p^2, q^2, p_\rho^1, q_\rho^1, p^3, q^3\}$. There exists a nonlinear map $T : C_X \to C_N$ that maps coefficients of the nonlinear terms in* (23) *about* $(0, \ldots, 0)$ *onto coefficients of the nonlinear terms in the normal forms* (7) and (8).

Proof. Perform the center manifold reduction on (19) with F as defined in (23) and $a_{13} = a_{21} = 1$. Term by term comparison between the reduced flow on the center manifold and the coefficients of the normal form equations (7) and (8) yields explicitly T, where $(dT)_{(0,\ldots,0)}$ is full rank. The proposition then follows from the implicit function theorem. □

Dividing a vector field by a scalar does not change its trajectories, it only changes the speed along which each trajectory is traversed. Moreover, it is straightforward to verify that Theorem 2.3 still holds when all coefficients except $q^1(0)$ are scaled. For instance, except for $q^1(0)$, divide the parameters (18) used to construct the cycle of Fig. 5 by 100, i.e. set

$$
\begin{aligned}
&c^1 = 0.01\lambda - 0.015\rho - 0.04N, \qquad c^2 = 0.013, \qquad c^3 = -0.09,\\
&c^5 = 0.5, \qquad p^1 = 0.012\lambda - 0.03\rho - N, \qquad p^9 = 0.04,\\
&p^2 = 0.04, \qquad p^3 = 0.04, \qquad q^1 = 0.008\lambda + 1, \qquad q^9 = 0.08.
\end{aligned}
$$

Next we perform a center manifold reduction on the cell system (19) and then apply Proposition 3.2. Solving for C_X yields

$$
\begin{aligned}
&a_{11} = -0.132091, \quad a_{12} = -0.130820, \quad a_{14} = 0.750809, \quad a_{22} = -0.750346,\\
&a_{23} = -0.097380, \quad a_{24} = -0.084128, \quad a_{25} = -0.079626, \quad a_{31} = -0.123358,\\
&a_{32} = -0.521642, \quad a_{33} = -0.257943, \quad a_{34} = 0.133102, \quad a_{35} = 0.159356.
\end{aligned} \tag{24}
$$

Numerical integration of (19) produces the cycle shown in Fig. 6. Simulating the trajectories for a longer time shows that each periodic solution appears for an approximately constant length of time.

The symmetries of SW1 can be visualized by magnifying the region of $x_{i2}(t)$ (see Fig. 7). As predicted by symmetry, two wave forms appear in the six cells. Cells 1 and 4 define the first wave form and oscillate with a half-period phase shift. The remaining cells describe the second wave form with cells 2 and 6 synchronized and cells 3 and 5 a half-period out-of-phase. Similarly, the second standing wave is visualized under magnification in Fig. 7. SW2 also has two wave forms. Cells 2, 3, 5 and 6 describe one wave with two cells synchronized and two cells a half-period out-of-phase. The synchronous cells 1 and 4 describe the second wave and, as predicted, they oscillate at twice the frequency of the other cells.

The details of this pattern of oscillation can be further explained by considering a Fourier series expansion of cell 3:

$$x_3(t) = a_0 + a_1 \mathrm{e}^{t\mathrm{i}} + a_2 \mathrm{e}^{2t\mathrm{i}} + a_3 \mathrm{e}^{3t\mathrm{i}} + a_4 \mathrm{e}^{4t\mathrm{i}} + \cdots .$$

Since the cell oscillates at twice the frequency, i.e. $x_3(t) = x_3(t + \frac{1}{2}T)$, it follows that $a_j = 0$ for all odd integers. Generically, $a_0 \neq 0$, which explains the nonzero mean in $x_3(t)$. Near bifurcation the other even Fourier coefficients are near zero, which explains the small amplitude of the double frequency oscillation.

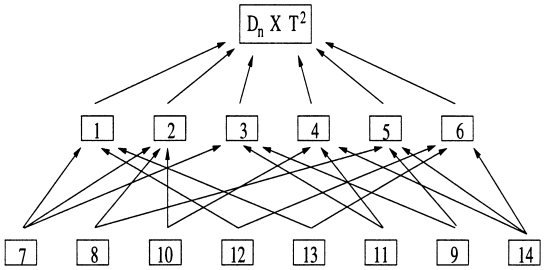

Fig. 10. Upper part of the lattice of isotropy subgroups of $\mathbf{D}_n \times \mathbf{T}^2$, up to conjugacy. The isotropy subgroups are listed in Table 9.

4. Hopf–Hopf mode interactions with $\mathbf{D}_n$-symmetry

In this section, we consider Hopf/Hopf mode interactions with $\mathbf{D}_n$-symmetry, $n \geq 5$. After a center manifold reduction we arrive at the reduced system of ODEs (5) with $z \in \mathbf{C}^4$. By an appropriate change of coordinates we can further assume that (5) is in Poincaré–Birkhoff normal form to any finite-order so that g is $\mathbf{D}_n \times \mathbf{T}^2$-equivariant. We can then choose coordinates $z = (z_1, z_2, z_3, z_4)$ such that the $\mathbf{D}_n \times \mathbf{T}^2$ action on $\mathbf{C}^4$ takes the following form. Let $\gamma = 2\pi/n \in \mathbf{Z}_n$ and κ be a fixed element in $\mathbf{D}_n \sim \mathbf{Z}_n$, and let $(\theta_1, \theta_2) \in \mathbf{T}^2$, then

$$\gamma(z_1, z_2, z_3, z_4) = (e^{i\gamma} z_1, e^{-i\gamma} z_2, e^{i\gamma} z_3, e^{-i\gamma} z_4), \qquad \kappa(z_1, z_2, z_3, z_4) = (z_2, z_1, z_4, z_3),$$
$$(\theta_1, \theta_2)(z_1, z_2, z_3, z_4) = (e^{i\theta_1} z_1, e^{i\theta_1} z_2, e^{i\theta_2} z_3, e^{i\theta_2} z_4).$$

4.1. The $\mathbf{D}_n \times \mathbf{T}^2$ lattice of isotropy subgroups

We look for heteroclinic cycles in the vector field g by inspection of the isotropy lattice. We consider the case $n \neq 0 \bmod 4$. When $n = 0 \bmod 4$, the existence and stability theorems that we prove for the $n \neq 0 \bmod 4$ case also hold. Define

$$\mathbf{Z}_2^{cn} = \begin{cases} \langle(\pi, \pi, \pi)\rangle & \text{if } n \text{ is even,} \\ 1 & \text{if } n \text{ is odd.} \end{cases}$$

Let $\mathbf{Z}_n(k, l, m) \equiv \{(k\gamma, l\gamma, m\gamma) \in \mathbf{Z}_n^3 : k, l, m \in \mathbf{Z}\}$, where γ is a generator of $\mathbf{Z}_n$, $\mathbf{S}^1(1, 0) \equiv \{(\theta, 0) \in \mathbf{T}^2 : \theta \in \mathbf{S}^1\}$, and $\mathbf{S}^1(0, 1) \equiv \{(0, \theta) \in \mathbf{T}^2 : \theta \in \mathbf{S}^1\}$. Part of the isotropy lattice of the action of $\mathbf{D}_n \times \mathbf{T}^2$ on $\mathbf{C}^4$ is given in Fig. 10, and the isotropy subgroups are listed in Table 9.

The isotropy lattice suggests the existence of three heteroclinic cycles.

1. A cycle connecting four types of standing waves: (2) → (4) through (10), (4) → (3) through (11), (3) → (5) through (9), and back to (2) through (8).
2. A cycle connecting two rotating waves (1) and (6) through (12) and (13).
3. A cycle connecting the standing waves as in (1), but instead (5) → (6) through (14), then (6) → (1) through (12) or (13), and (1) → (2) through (7). This cycle connects standing waves and rotating waves.

In the following, we sketch the existence and asymptotic stability of the first two cycles. The existence of the third cycle is more difficult to establish since the connecting fixed-point subspaces (7) and (14) are four-dimensional. It is likely that generically these cycles do not exist.

4.2. $\mathbf{D}_n$-invariants and $\mathbf{D}_n$-equivariants

In this section, we compute normal form equations for $\mathbf{D}_n \times \mathbf{T}^2$-equivariant smooth germs on $\mathbf{C}^4$. First, let

Table 9
Isotropy subgroups of the $\mathbf{D}_n \times \mathbf{T}^2$-action on $\mathbf{C}^4$ from the lattice in Fig. 10

	Isotropy subgroup	Fixed-point subspace
(1)	$\mathbf{Z}_n(1,-1,0) \times \mathbf{S}^1(0,1)$	$(z,0,0,0)$
(2)	$\mathbf{Z}_2(\kappa) \times \mathbf{Z}_2^{cn} \times \mathbf{S}^1(0,1)$	$(z,z,0,0)$
(3)	$\mathbf{Z}_2(\kappa,\pi,0) \times \mathbf{Z}_2^{cn} \times \mathbf{S}^1(0,1)$	$(z,-z,0,0)$
(4)	$\mathbf{Z}_2(\kappa,0,\pi) \times \mathbf{Z}_2^{cn} \times \mathbf{S}^1(1,0)$	$(0,0,z,-z)$
(5)	$\mathbf{Z}_2(\kappa) \times \mathbf{Z}_2^{cn} \times \mathbf{S}^1(1,0)$	$(0,0,z,z)$
(6)	$\mathbf{Z}_n(1,0,1) \times \mathbf{S}^1(1,0)$	$(0,0,0,z)$
(7)	$\mathbf{S}^1(0,1)$	$(z_1,z_2,0,0)$
(8)	$\mathbf{Z}_2(\kappa) \times \mathbf{Z}_2^{cn}$	(z_1,z_1,z_3,z_3)
(9)	$\mathbf{Z}_2(\kappa,\pi,0) \times \mathbf{Z}_2^{cn}$	$(z_1,-z_1,z_3,z_3)$
(10)	$\mathbf{Z}_2(\kappa,0,\pi) \times \mathbf{Z}_2^{cn}$	$(z_1,z_1,z_3,-z_3)$
(11)	$\mathbf{Z}_2(\kappa,\pi,\pi) \times \mathbf{Z}_2^{cn}$	$(z_1,-z_1,z_3,-z_3)$
(12)	$\mathbf{Z}_n(1,-1,1)$	$(z_1,0,0,z_4)$
(13)	$\mathbf{Z}_n(1,1,1)$	$(0,z_2,0,z_4)$
(14)	$\mathbf{S}^1(1,0)$	$(0,0,z_3,z_4)$

$$m = \begin{cases} n & \text{if } n \text{ is odd,} \\ \frac{1}{2}n & \text{if } n \text{ is even.} \end{cases}$$

Proposition 4.1. *Every smooth $\mathbf{D}_n \times \mathbf{T}^2$-invariant germ $f : \mathbf{C}^4 \to \mathbf{R}$ is a function of $N_1 = |z_1|^2 + |z_2|^2$, $N_2 = |z_3|^2 + |z_4|^2$, $\Delta_1 = \delta_1^2$, $\Delta_2 = \delta_2^2$, $\Delta_{12} = \delta_1\delta_2$, $x = z_1\bar{z}_2z_3\bar{z}_4 + \bar{z}_1z_2\bar{z}_3z_4$.*

$$\mathrm{Re}(I_0), \mathrm{Re}(I_1), \ldots, \mathrm{Re}(I_m), \delta_j\,\mathrm{Im}(I_0), \ldots, \delta_j\,\mathrm{Im}(I_m),$$

where $j = 1, 2$, $I_k = (z_1\bar{z}_2)^{m-k}(z_3\bar{z}_4)^k$ and $\delta_1 = |z_2|^2 - |z_1|^2$, $\delta_2 = |z_4|^2 - |z_3|^2$.

The proof of Proposition 4.1 is similar to that of Proposition 2.1 for $\mathbf{D}_6 \times \mathbf{S}^1$-invariants and is omitted for brevity.

Proposition 4.2. *Let $f : \mathbf{C}^4 \to \mathbf{C}^4$ commute with the action of $\mathbf{D}_n \times \mathbf{T}^2$. The general $\mathbf{D}_n \times \mathbf{T}^2$-equivariant mapping $f = (f_1, f_2, f_3, f_4)$ is given by*

$$\begin{aligned} f(z,\lambda,\mu) = {} & C^1 \begin{bmatrix} z_1 \\ z_2 \\ z_3 \\ z_4 \end{bmatrix} + (C^3\delta_1 + C^5\delta_2) \begin{bmatrix} z_1 \\ -z_2 \\ z_3 \\ -z_4 \end{bmatrix} + (C^7 + C^9\delta_1 + C^{11}\delta_2) \begin{bmatrix} z_2v_{34} \\ z_1\bar{v}_{34} \\ z_4v_{12} \\ z_3\bar{v}_{12} \end{bmatrix} \\ & + C^{13} \begin{bmatrix} z_1v_{12}\bar{v}_{34} \\ z_2\bar{v}_{12}v_{34} \\ z_3\bar{v}_{12}v_{34} \\ z_4v_{12}\bar{v}_{34} \end{bmatrix} + \sum_{i=0}^{m-1}\sum_{j=0}^{2} D_{j+1}^{2i+1}\delta_j \begin{bmatrix} \bar{v}_{12}^{m-1-i}\bar{v}_{34}^i z_2 \\ v_{12}^{m-1-i}v_{34}^i z_1 \\ \bar{v}_{34}^{m-1-i}\bar{v}_{12}^i z_4 \\ v_{34}^{m-1-i}v_{12}^i z_3 \end{bmatrix}, \end{aligned} \tag{25}$$

where $\delta_0 = 1$, $v_{12} = z_1\bar{z}_2$, $v_{34} = z_3\bar{z}_4$, C^j and D_l^j are complex-valued $\mathbf{D}_n \times \mathbf{T}^2$-invariant functions of two parameters λ and μ, and

Table 10
Expansion of the branching equations to lowest order in u for each maximal isotropy solution

	Solution	Orbit type	Expansion
(1)	RW_{ω_1}	$(u, 0, 0, 0)$	$\lambda = \dfrac{a^3 - a^1_{N_1}}{a^1_\lambda} u^2$
(2)	$\mathrm{SW1}_{\omega_1}$	$(u, u, 0, 0)$	$\lambda = -\dfrac{2a^1_{N_1}}{a^1_\lambda} u^2$
(3)	$\mathrm{SW2}_{\omega_1}$	$(u, -u, 0, 0)$	$\lambda = -\dfrac{2a^1_{N_1}}{a^1_\lambda} u^2$
(4)	$\mathrm{SW2}_{\omega_2}$	$(0, 0, u, -u)$	$\lambda = -\dfrac{2b^1_{N_2}}{b^1_\lambda} u^2$
(5)	$\mathrm{SW1}_{\omega_2}$	$(0, 0, u, u)$	$\lambda = -\dfrac{2b^1_{N_2}}{b^1_\lambda} u^2$
(6)	RW_{ω_2}	$(0, 0, u, 0)$	$\lambda = \dfrac{b^5 - b^1_{N_2}}{b^1_\lambda} u^2$

$$C^j = \begin{bmatrix} a^j + \mathrm{i}a^{j+1} \\ a^j + \mathrm{i}a^{j+1} \\ b^j + \mathrm{i}b^{j+1} \\ b^j + \mathrm{i}b^{j+1} \end{bmatrix}, \qquad D^j_l = \begin{bmatrix} q^j_l + \mathrm{i}q^{j+1}_l \\ q^j_l + \mathrm{i}q^{j+1}_l \\ r^j_l + \mathrm{i}r^{j+1}_l \\ r^j_l + \mathrm{i}r^{j+1}_l \end{bmatrix}.$$

A proof of Proposition 4.2 is similar to that of Proposition 2.2 for $\mathbf{D}_6 \times \mathbf{S}^1$-equivariants and is omitted for brevity.

4.3. Branching equations

Consider a general $\mathbf{D}_n \times \mathbf{T}^2$-equivariant vector field f on $\mathbf{C}^4$ that depends on two parameters λ and μ. Assume that at the origin the vector field has a nonresonant Hopf–Hopf mode interaction when $\lambda = \mu = 0$ and that the eigenvalues of $(df)_0$ are $\omega_1\mathrm{i}$, $\omega_2\mathrm{i}$, where ω_1 and ω_2 are not rationally related. This implies that $a^1(0) = b^1(0) = 0$, $a^2(0) = \omega_1$, and $b^2(0) = \omega_2$.

On solving the amplitude equations corresponding to $f|\mathrm{Fix}(\Sigma)$, we find branches of periodic solutions bifurcating from the trivial equilibrium for each maximal isotropy subgroup Σ of $\mathbf{D}_n \times \mathbf{T}^2$. For each Hopf bifurcation, there is one rotating wave with isotropy subgroup $\mathbf{Z}_n \times \mathbf{Z}_n \times \mathbf{S}^1$ denoted RW and two standing waves, one with isotropy subgroup $\mathbf{Z}_2(\kappa) \times \mathbf{Z}_2^{cn} \times \mathbf{S}^1$ denoted SW1 and one with isotropy subgroup $\mathbf{Z}_2(\kappa, \pi) \times \mathbf{Z}_2^{cn} \times \mathbf{S}^1$ denoted SW2 where $\mathbf{S}^1 = \mathbf{S}^1(0, 1)$ for the ω_1 Hopf bifurcation and $\mathbf{S}^1 = \mathbf{S}^1(1, 0)$ for the ω_2 Hopf bifurcation (see Table 10).

Using the isotypic decomposition $\mathbf{C}^4 = V_1 \oplus V_2 \oplus V_3 \oplus V_4$, given by each maximal isotropy subgroup Σ, the stability of the bifurcating periodic solution is determined by $\mathrm{trace}(df)|V_j$ for all j (see Table 11). Since $\dim \Sigma = 1$ at maximal isotropy solutions, the action of $\mathbf{D}_n \times \mathbf{T}^2/\Sigma$ on the tangent space forces (df) to have a zero eigenvalue in $V_1 = \mathrm{Fix}(\Sigma)$. The action on the other irreducible representations is by a rotation so generically the eigenvalues are complex.

Since $f_1 = f_2 \circ \kappa$, we can write df at the origin in complex coordinates as

$$df(W) = \left[\sum_{i=1}^{4} \left[\frac{\partial f_i}{\partial z_1} w_i + \frac{\partial f_i}{\partial \bar{z}_1} \bar{w}_i \right], \ldots, \sum_{i=1}^{4} \left[\frac{\partial f_i}{\partial z_4} w_i + \frac{\partial f_i}{\partial \bar{z}_4} \bar{w}_i \right] \right],$$

Table 11
Irreducible representations of the tangent space at maximal isotropy solutions[a]

	Solution	V_1	V_2	V_3	V_4
(1)	RW_{ω_1}	$(w, 0, 0, 0)$	$(0, w, 0, 0)$	$(0, 0, w, 0)$	$(0, 0, 0, w)$
(2)	$SW1_{\omega_1}$	$(w, w, 0, 0)$	$(w, -w, 0, 0)$	$(0, 0, w, w)$	$(0, 0, w, -w)$
(3)	$SW2_{\omega_1}$	$(w, -w, 0, 0)$	$(w, w, 0, 0)$	$(0, 0, w, -w)$	$(0, 0, w, w)$
(4)	$SW2_{\omega_2}$	$(0, 0, w, -w)$	$(0, 0, w, w)$	$(w, -w, 0, 0)$	$(w, w, 0, 0)$
(5)	$SW1_{\omega_2}$	$(0, 0, w, w)$	$(0, 0, w, -w)$	$(w, w, 0, 0)$	$(w, -w, 0, 0)$
(6)	RW_{ω_2}	$(0, 0, w, 0)$	$(0, 0, 0, w)$	$(w, 0, 0, 0)$	$(0, w, 0, 0)$

[a]Note that $(df)|V_1$ has one null vector.

Table 12
Real part of trace of $(df)|V_i$ for each maximal isotropy solution up to a positive constant

	Solution	V_1	V_2	V_3	V_4
(1)	RW_{ω_1}	$\frac{\partial}{\partial z_1} f_1$	$\frac{\partial}{\partial z_2} f_2$	$\frac{\partial}{\partial z_3} f_3$	$\frac{\partial}{\partial z_4} f_4$
(2)	$SW1_{\omega_1}$	$\frac{\partial}{\partial z_1}(f_1 + f_2)$	$\frac{\partial}{\partial z_1}(f_1 - f_2)$	$\frac{\partial}{\partial z_3}(f_3 + f_4)$	$\frac{\partial}{\partial z_3}(f_3 - f_4)$
(3)	$SW2_{\omega_1}$	$\frac{\partial}{\partial z_1}(f_1 - f_2)$	$\frac{\partial}{\partial z_1}(f_1 + f_2)$	$\frac{\partial}{\partial z_3}(f_3 - f_4)$	$\frac{\partial}{\partial z_3}(f_3 + f_4)$
(4)	$SW2_{\omega_2}$	$\frac{\partial}{\partial z_3}(f_3 - f_4)$	$\frac{\partial}{\partial z_3}(f_3 + f_4)$	$\frac{\partial}{\partial z_1}(f_1 - f_2)$	$\frac{\partial}{\partial z_1}(f_1 + f_2)$
(5)	$SW1_{\omega_2}$	$\frac{\partial}{\partial z_3}(f_3 + f_4)$	$\frac{\partial}{\partial z_3}(f_3 - f_4)$	$\frac{\partial}{\partial z_1}(f_1 + f_2)$	$\frac{\partial}{\partial z_1}(f_1 - f_2)$
(6)	RW_{ω_2}	$\frac{\partial}{\partial z_3} f_3$	$\frac{\partial}{\partial z_4} f_4$	$\frac{\partial}{\partial z_1} f_1$	$\frac{\partial}{\partial z_2} f_2$

Table 13
Explicit computation of trace$(df)|V_1$ at each maximal isotropy solution

	z	V_1
(1)	$(u, 0, 0, 0)$	$a^1 + (a^1_{N_1} - 2a^3)u^2 + (2a^1_{\Delta_1} - a^3_{N_1})u^4 - 2a^3_{\Delta_1} u^6$
(2)	$(u, u, 0, 0)$	$a^1 + 2a^1_{N_1} u^2 + mq^1_1 u^{2(m-1)} + 2m(q^1_1)_{\mathrm{Re}(I_0)}\, u^{4m-2} + 2[(q^1_1)_{N_1} - q^1_2 + ma^1_{\mathrm{Re}(I_0)}]u^{2m}$
(3)	$(u, -u, 0, 0)$	$a^1 + 2a^1_{N_1} u^2 + (-1)^m mq^1_1 u^{2(m-1)} + 2m(q^1_1)_{\mathrm{Re}(I_0)}\, u^{4m-2} + 2(-1)^{m-1}[(-1)^{m-1} ma^1_{\mathrm{Re}(I_0)} - (q^1_1)_{N_1} + q^1_2]u^{2m}$
(4)	$(0, 0, u, -u)$	$b^1 + 2b^1_{N_2} u^2 + (-1)^m mr^1_1 u^{2(m-1)} + 2m(r^1_1)_{\mathrm{Re}(I_m)}\, u^{4m-2} + 2(-1)^m[(r^1_1)_{N_2} + r^1_2 + mb^1_{\mathrm{Re}(I_m)}]u^{2m}$
(5)	$(0, 0, u, u)$	$b^1 + 2b^1_{N_2} u^2 + mr^1_1 u^{2(m-1)} + 2m(r^1_1)_{\mathrm{Re}(I_m)}\, u^{4m-2} + 2[(r^1_1)_{N_2} - r^1_2 + mb^1_{\mathrm{Re}(I_m)}]u^{2m}$
(6)	$(0, 0, u, 0)$	$b^1 + (b^1_{N_2} - 2b^5)u^2 + (2b^1_{\Delta_2} - b^5_{N_2} u)^4 - 2b^5_{\Delta_2} u^6$

where $W = (w_1, w_2, w_3, w_4) \in \mathbf{C}^4$. The relevant traces are listed in Table 12 for each maximal isotropy solution. Their signs appear in Tables 13–15 for each maximal isotropy solution and each irreducible representation in the isotypic decomposition.

The real part of the eigenvalues on the irreducible V_i at each maximal isotropy solution (j) is given by $\epsilon_{ij} u^2 + \cdots$. The ϵ_{ij} are listed in (26).

Table 14
Explicit computation of trace$(df)|V_2$ at each maximal isotropy solution

	z	V_2
(1)	$(u,0,0,0)$	$a^1+a^3u^2$
(2)	$(u,u,0,0)$	$a^1-2a^3u^2-mq_1^1u^{2(m-1)}$
(3)	$(u,-u,0,0)$	$a^1-2a^3u^2+(-1)^m mq_1^1u^{2(m-1)}$
(4)	$(0,0,u,-u)$	$b^1-2b^5u^2+(-1)^m mr_1^1u^{2(m-1)}$
(5)	$(0,0,u,u)$	$b^1-2b^5u^2-mr_1^1u^{2(m-1)}$
(6)	$(0,0,u,0)$	$b^1+b^5u^2$

$$
\begin{aligned}
&\epsilon_{11}=(a^1_{N_1}-a^3), \qquad \epsilon_{12}=\epsilon_{13}=2a^1_{N_1}, \qquad \epsilon_{14}=\epsilon_{15}=2b^1_{N_2},\\
&\epsilon_{16}=(b^1_{N_2}-b^5), \qquad \epsilon_{21}=-\epsilon_{22}=-\epsilon_{23}=2a^3, \qquad \epsilon_{26}=-\epsilon_{24}=-\epsilon_{25}=2b^5,\\
&\epsilon_{31}=\frac{[(b^1_{N_1}-b_3)a^1_\lambda-b^1_\lambda(a^1_{N_1}-a^3)]}{a^1_\lambda}, \qquad \epsilon_{32}=\frac{[(2b^1_{N_1}+b^7)a^1_\lambda-2b^1_\lambda a^1_{N_1}]}{a^1_\lambda}, \qquad \epsilon_{33}=\epsilon_{32},\\
&\epsilon_{34}=\frac{[(2a^1_{N_2}+a^7)b^1_\lambda-2a^1_\lambda b^1_{N_2}]}{b^1_\lambda}, \qquad \epsilon_{35}=\epsilon_{34}, \qquad \epsilon_{36}=-\frac{[(b^1_{N_2}-b^5)a^1_\lambda+(a^1_{N_2}-a^5)b^1_\lambda]}{b^1_\lambda},\\
&\epsilon_{41}=\frac{[(b^1_{N_1}+b^3)a^1_\lambda-b^1_\lambda(a^1_{N_1}-a^3)]}{a^1_\lambda}, \qquad \epsilon_{42}=\frac{[(2b^1_{N_1}-b^7)a^1_\lambda-2b^1_\lambda a^1_{N_1}]}{a^1_\lambda}, \qquad \epsilon_{43}=\epsilon_{42},\\
&\epsilon_{44}=\frac{[(2a^1_{N_2}-a^7)b^1_\lambda-2a^1_\lambda b^1_{N_2}]}{b^1_\lambda}, \qquad \epsilon_{45}=\epsilon_{44}, \qquad \epsilon_{46}=\frac{[(a^1_{N_2}+a^5)b^1_\lambda-(b^1_{N_2}-b^5)a^1_\lambda]}{b^1_\lambda}.
\end{aligned}
\tag{26}
$$

4.4. Existence and stability of cycles

We show the existence of a heteroclinic cycle by verifying that trajectories in the two-dimensional fixed-point subspaces are bounded and that no other equilibria exist. In order to do this, we need the following definitions:

$$
\begin{aligned}
&\epsilon_1=\frac{a^1_{N_2}b^1_\lambda}{b^1_{N_2}a^1_\lambda}+\frac{b^1_{N_1}a^1_\lambda}{a^1_{N_1}b^1_\lambda}, \qquad \epsilon_2=\frac{(2a^1_{N_2}-a^7)b^1_\lambda}{2b^1_{N_2}a^1_\lambda}+\frac{(2b^1_{N_1}-b^7)a^1_\lambda}{2a^1_{N_1}b^1_\lambda},\\
&\epsilon_3=\frac{(2a^1_{N_2}-a^7)b^1_\lambda}{2b^1_{N_2}a^1_\lambda}+\frac{(2b^1_{N_1}-b^7)a^1_\lambda}{2a^1_{N_1}b^1_\lambda}, \qquad \epsilon_4=\frac{(2a^1_{N_2}+a^7)b^1_\lambda}{2b^1_{N_2}a^1_\lambda}+\frac{(2b^1_{N_1}+b^7)a^1_\lambda}{2a^1_{N_1}b^1_\lambda}.
\end{aligned}
$$

Table 15
Explicit computation of trace$(df)|V_3$ and trace$(\mathrm{d}f)|_{V_4}$ at each maximal isotropy solution

	z	V_3	V_4
(1)	$(u,0,0,0)$	$b^1-b^3u^2$	$b^1+b^3u^2$
(2)	$(u,u,0,0)$	$b^1+b^7u^2+r_1^{2m-1}u^{2(m-1)}$	$b^1-b^7u^2+r_1^{2m-1}u^{2(m-1)}$
(3)	$(u,-u,0,0)$	$b^1+b^7u^2+(-1)^{m-1}r_1^{2m-1}u^{2(m-1)}$	$b^1-b^7u^2+(-1)^{m-1}r_1^{2m-1}u^{2(m-1)}$
(4)	$(0,0,u,-u)$	$a^1-a^7u^2+(-1)^m q_1^{2m-1}u^{2(m-1)}$	$a^1-a^7u^2+(-1)^m q_1^{2m-1}u^{2(m-1)}$
(5)	$(0,0,u,u)$	$a^1+a^7u^2+q_1^{2m-1}u^{2(m-1)}$	$a^1+a^7u^2-q_1^{2m-1}u^{2(m-1)}$
(6)	$(0,0,u,0)$	$a^1-a^5u^2$	$a^1+a^5u^2$

Table 16
Sign of the real part of the eigenvalues at each standing wave solution

	Solution	Fix($\mathbf{Z}_2(\kappa)$)	Fix($\mathbf{Z}_2(\kappa,\pi,0)$)	Fix($\mathbf{Z}_2(\kappa,0,\pi)$)	Fix($\mathbf{Z}_2(\kappa,\pi,\pi)$)
(2)	$SW1_{\omega_1}$	$\operatorname{sgn}(\epsilon_{32})$			$\operatorname{sgn}(\epsilon_{42})$
(3)	$SW2_{\omega_2}$	$\operatorname{sgn}(\epsilon_{35})$	$\operatorname{sgn}(\epsilon_{45})$		
(4)	$SW2_{\omega_1}$		$\operatorname{sgn}(\epsilon_{43})$	$\operatorname{sgn}(\epsilon_{33})$	
(5)	$SW1_{\omega_2}$			$\operatorname{sgn}(\epsilon_{34})$	$\operatorname{sgn}(\epsilon_{44})$

Theorem 4.3. *Let $\mu = 0$. For $\lambda > 0$, there exists a branch of robust heteroclinic cycles in* (25) *consisting of trajectories that connect* $SW1_{\omega_1}$ *to* $SW2_{\omega_2}$, $SW2_{\omega_2}$ *to* $SW2_{\omega_1}$, $SW2_{\omega_1}$ *to* $SW1_{\omega_2}$, *and* $SW1_{\omega_2}$ *to* $SW1_{\omega_1}$.

$$a^1_\lambda(0) > 0, \qquad b^1_\lambda(0) > 0, \qquad \epsilon_{1i} < 0, \quad i = 2,3,4,5,$$

and

$$\begin{aligned} &\operatorname{sgn}\epsilon_{32} = \operatorname{sgn}\epsilon_{45}, \qquad \operatorname{sgn}\epsilon_{32} = -\operatorname{sgn}\epsilon_{35}, \qquad \operatorname{sgn}\epsilon_{33} = -\operatorname{sgn}\epsilon_{34}, \qquad \operatorname{sgn}\epsilon_{44} = -\operatorname{sgn}\epsilon_{42},\\ &\operatorname{sgn}\epsilon_{45} = -\operatorname{sgn}\epsilon_{43}, \qquad \epsilon_i > -2, \quad i = 1,\dots,4. \end{aligned} \tag{27}$$

Proof. Since $a^1_\lambda, b^1_\lambda > 0$ when λ is positive, branches of solutions with maximal isotropy subgroup bifurcate from the origin. Table 16 shows the sign of the real part of the eigenvalues of the Jacobian at the standing waves periodic solutions. In order to obtain a cycle, the sign of adjacent eigenvalues must be alternately positive and negative so that saddle–sink connections can be established in each two-dimensional fixed-point subspace. This is satisfied by (27). The boundedness of solutions and the nonexistence of other equilibria in the fixed-point subspaces is guaranteed by $\epsilon_k > -2$ ($k = 1,2,3,4$) and Proposition 2.4. □

Theorem 4.4. *The branch of heteroclinic cycles between the different types of standing waves found in Theorem* 4.3 *generically consists of asymptotically stable cycles if the following conditions are satisfied*:

$$\begin{aligned} &\epsilon_{22} < 0, \qquad \epsilon_{25} < 0, \qquad \min(-\epsilon_{32}, \epsilon_{42} - \epsilon_{22})\min(-\epsilon_{45}, \epsilon_{35} - \epsilon_{25}) > \epsilon_{42}\epsilon_{35},\\ &\min(-\epsilon_{42}, \epsilon_{32} - \epsilon_{22})\min(-\epsilon_{35}, \epsilon_{45} - \epsilon_{25}) > \epsilon_{32}\epsilon_{45}. \end{aligned} \tag{28}$$

Proof. Follows from Theorem 2.7 of Krupa and Melbourne [19]. □

Define

$$\epsilon_5 = \frac{(a^1_{N_2} + a^5)b^1_\lambda}{(b^1_{N_2} - b^5)a^1_\lambda} + \frac{(b^1_{N_1} + b^3)a^1_\lambda}{(a^1_{N_1} - a^3)b^1_\lambda}, \qquad \epsilon_6 = \frac{(a^1_{N_2} - a^5)b^1_\lambda}{(b^1_{N_2} - b^5)a^1_\lambda} + \frac{(b^1_{N_1} - b^3)a^1_\lambda}{(a^1_{N_1} - a^3)b^1_\lambda}.$$

Theorem 4.5. *Let $\mu = 0$. For $\lambda > 0$, there exists a branch of robust heteroclinic cycles in* (25) *connecting rotating wave* (1) *with rotating wave* (6) *through the fixed-point subspaces* (12) *and* (13) *if*

$$\begin{aligned} &a^1_\lambda(0) > 0, \qquad b^1_\lambda(0) > 0, \qquad \epsilon_{1i} < 0, \quad i = 1,6,\\ &\operatorname{sgn}(\epsilon_{31}) = \operatorname{sgn}(\epsilon_{36}) = -\operatorname{sgn}(\epsilon_{41}) = -\operatorname{sgn}(\epsilon_{46}), \qquad \epsilon_5 > -2, \quad \epsilon_6 > -2. \end{aligned} \tag{29}$$

Proof. Similar to the proof of Theorem 4.1 of Melbourne et al. [22]. □

Theorem 4.6. *The branch of heteroclinic cycles between rotating waves found in Theorem* 4.5 *consists of asymptotically stable cycles if*

$$\epsilon_{21} < 0, \qquad \epsilon_{26} < 0, \qquad \min(-\epsilon_{31}, \epsilon_{41} - \epsilon_{21})\min(-\epsilon_{36}, \epsilon_{46} - \epsilon_{26}) > \epsilon_{41}\epsilon_{46},$$
$$\min(-\epsilon_{41}, \epsilon_{31} - \epsilon_{21})\min(-\epsilon_{46}, \epsilon_{36} - \epsilon_{26}) > \epsilon_{31}\epsilon_{36}.$$

Proof. Similar to the proof of Theorem 4.3 of Melbourne et al. [22]. □

A heteroclinic cycle involving standing and rotating waves is more difficult to establish. For instance, consider tentatively a cycle connecting rotating wave (1) with standing wave (2) or (3) through the fixed-point subspace (7). In this case, when the system is transformed to polar coordinates, the equations of motion do not decouple into amplitude/phase equations. Instead, we obtain

$$\dot{\rho}_1 = a^1\rho_1 + a^3\delta_1\rho_1 + \sum_{j=0}^{2}\delta_j\rho_1^{m-1}\rho_2^m[q_{j+1}^1\cos(m-2)\phi - r_{j+1}^1\sin(m-2)\phi],$$
$$\dot{\rho}_2 = a^1\rho_2 - a^3\delta_1\rho_2 + \sum_{j=0}^{2}\delta_j\rho_2^{m-1}\rho_1^m[q_{j+1}^1\cos(m-2)\phi + r_{j+1}^1\sin(m-2)\phi], \tag{30}$$

where $\phi = \theta_1 - \theta_2$, and ρ_1 and ρ_2 are amplitude variables. The dynamics in the four-dimensional space $(z_1, z_2, 0, 0)$ is given by $(\dot{\rho}_1, \dot{\rho}_2, \dot{\phi})$. Therefore, the existence of a connection between (1) and either (2) or (3) cannot be determined by the previous methods. The existence of a saddle–sink connection in this context is unlikely.

4.5. Visualization of heteroclinic cycles in coupled cell system

We now visualize the heteroclinic cycles from the Hopf/Hopf interaction in a $\mathbf{D}_5$-symmetric coupled cell system without computing the center manifold reduction. We illustrate the method using the heteroclinic cycles in $\mathbf{D}_5 \times \mathbf{T}^2$-equivariant Poincaré–Birkhoff normal form. For a $\mathbf{D}_5$-symmetric cell system to have a Hopf/Hopf mode interaction with eight-dimensional real center eigenspace, the cells must be at least of dimension 4 — two dimensions for each Hopf bifurcation. If the dimension of the cell is lower than 4, the interaction of Hopf modes is impossible since the linearization can have at most one pair of complex eigenvalues with eigenspace invariant under the standard action of $\mathbf{D}_n$. We set the size to $k = 4$, so the ring of five cells is 20-dimensional. We use the fact that the smooth mapping from $\mathbf{D}_5$-symmetric cell systems with Hopf/Hopf mode interaction to $\mathbf{D}_5 \times \mathbf{T}^2$-equivariant normal form is onto. This map is given by the composition of the center manifold reduction with the Poincaré–Birkhoff normal form transformations. Here we assume that all possible couplings (both linear and nonlinear) are allowed between the cells.

Let $z = (z_1(t), z_2(t), z_3(t), z_4(t))$ denote the evolution of the heteroclinic cycle found in the normal form equations (25). Define vectors $V_1(t) = z$ and $V_2(t)$ to be the solution of a system of ODEs of the form

$$\frac{\mathrm{d}V_2}{\mathrm{d}t} = -rI_{12}V_2,$$

where r is a positive, real-valued scaling factor, and I_{12} a 12×12 identity matrix. Observe that $V_1 \in \mathbf{R}^8$ and $V_2 \in \mathbf{R}^{12}$. Next, embed the cycle in $\mathbf{R}^{20}$ by defining

$$V(t) = [V_1, V_2].$$

Table 17
Symmetries of solutions in a coupled cell system with five cells

Solution	Isotropy subgroup	Pattern of solution
Trivial	$\mathbf{D}_5 \times \mathbf{T}^2$	$X = (0, 0, 0, 0, 0)$
RW	$\mathbf{Z}_n(1, -1, 0) \times \mathbf{S}^1(0, 1)$	$X(t) = (X_1(t), X_2(t), X_3(t), X_4(t), X_5(t))$, where $X_{i+1}(t) = X_i(t + \frac{1}{5})$, i is taken mod 5
SW1	$\mathbf{Z}_2(\kappa) \times \mathbf{Z}_2^{cn} \times \mathbf{S}^1(0, 1)$	$X(t) = (X_1(t), X_2(t), X_3(t), X_3(t), X_2(t))$
SW2	$\mathbf{Z}_2(\kappa, \pi, 0) \times \mathbf{Z}_2^{cn} \times \mathbf{S}^1(0, 1)$	$X(t) = (X_1(t), X_2(t), X_3(t), X_3(t + \frac{1}{2}), X_2(t + \frac{1}{2}))$, where $X_1(t) = X_1(t + \frac{1}{2})$

It follows that V_1 is asymptotically stable inside $\mathbf{R}^{20}$ and the flow restricted to the center eigenspace is exactly V_1. We then map V to a vector solution X of a coupled cell system by applying a transformation $X = PQV$ similar to the one of Section 3. However, before doing the transformation, we need to break the $\mathbf{T}^2$-symmetry of the normal form using $\mathbf{D}_5$-equivariant terms since $\mathbf{T}^2$ is not a symmetry of the coupled cell system. The choice of the $\mathbf{D}_5$-equivariant term is arbitrary — some choices are better than others. Consequently, some quantitative features of the cell dynamics may not be exact. However, the numerical simulations describe well the predicted qualitative aspects of the dynamics.

Table 17 shows the restrictions that the symmetries impose on the periodic solutions of the cell system. We now perform the transformation with $V(t)$ as defined above and with $r = 1$. The results are shown in Figs. 11–13. Fig. 11 shows the heteroclinic cycle joining standing waves SW1 and SW2 as in Theorem 4.3. The left time series shows the evolution of the cells in the variables of one mode and the right time series shows the evolution of the other mode. Fig. 12 depicts the enlarged region $t \in [1200, 1400]$ of Fig. 11. The time series shows the double frequency oscillation of cell 1 when the cycle approaches the standing wave SW2. Fig. 13 shows a cycle connecting rotating waves. The time series on the left and right depict the first and second mode of oscillation in the cycle. Observe the phase shift of one-fifth period between consecutive cells.

Finally, Fig. 14 shows cycling behavior between SW1, SW2, and RW in a coupled cell system with $\mathbf{D}_5$-symmetry. The trajectory approaches RW when all five cells show the same amplitude, it is near SW2 when one cell has oscillation amplitude close to zero and it is near SW1 otherwise.

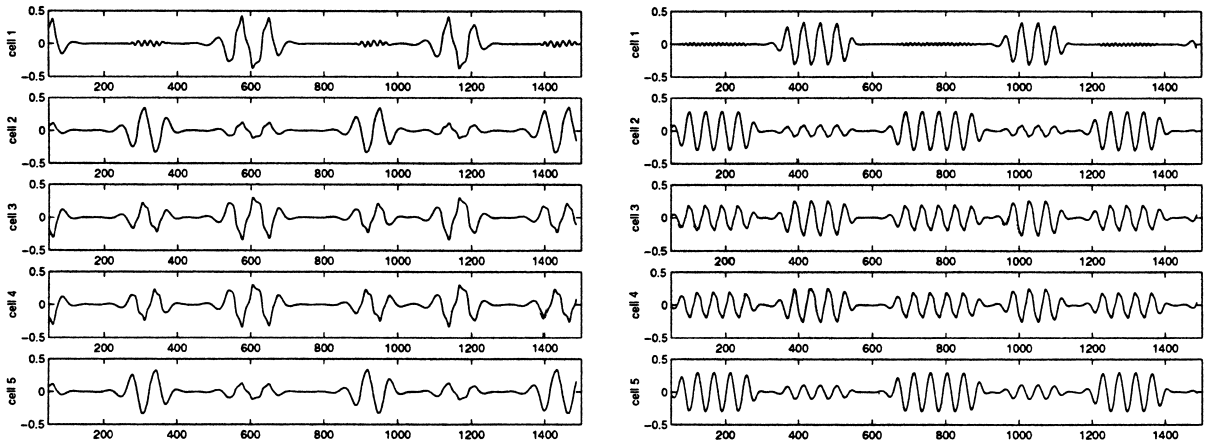

Fig. 11. Heteroclinic cycle connecting standing waves in the two modes of a Hopf/Hopf mode interaction. (Left) Cycle shown in a coordinate of the first mode. (Right) Cycle shown in a coordinate of the second mode.

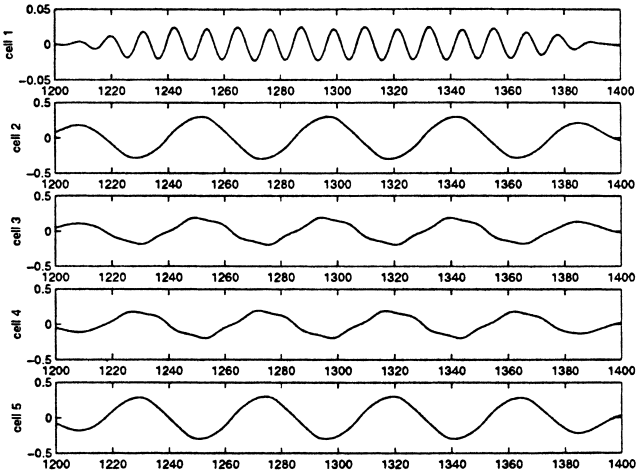

Fig. 12. Enlargement of Fig. 11 showing double frequency oscillation observed in cell 1 of a second mode coordinate.

The numerical simulations are performed with

$$f(z) = (f_1(z),\, f_2(z),\, f_3(z),\, f_4(z))$$
$$= \begin{bmatrix} ((a^1 + \mathrm{i}a^2) + (a^3 + \mathrm{i}a^4)\delta_1 + (a^5 + \mathrm{i}a^6)\delta_2)z_1 + (a^7 z_3\bar{z}_4 + (q_1^1 + \mathrm{i}q_1^2)(\bar{z}_1 z_2)^4)z_2 + p^1(z) \\ ((a^1 + \mathrm{i}a^2) - (a^3 + \mathrm{i}a^4)\delta_1 - (a^5 + \mathrm{i}a^6)\delta_2)z_2 + (a^7 z_4\bar{z}_3 + (q_1^1 + \mathrm{i}q_1^2)(\bar{z}_2 z_1)^4)z_1 + p^1(\kappa z) \\ ((b^1 + \mathrm{i}b^2) + (b^3 + \mathrm{i}b^4)\delta_1 + (b^5 + \mathrm{i}b^6)\delta_2)z_3 + (b^7 z_1\bar{z}_2 + (r_1^1 + \mathrm{i}r_1^2)(\bar{z}_3 z_4)^4)z_4 + p^3(z) \\ ((b^1 + \mathrm{i}b^2) - (b^3 + \mathrm{i}b^4)\delta_1 - (b^5 + \mathrm{i}b^6)\delta_2)z_4 + (b^7 z_2\bar{z}_1 + (r_1^1 + \mathrm{i}r_1^2)(\bar{z}_4 z_3)^4)z_3 + p^3(\kappa z), \end{bmatrix} \quad (31)$$

where

$$a^1 = p_\lambda^1\lambda + a_{N_1}^1 N_1 + a_{N_2}^1 N_2, \qquad b^1 = p_\lambda^2\lambda + b_{N_1}^1 N_1 + b_{N_2}^1 N_2,$$
$$p^1 = p_1^1\bar{z}_1^4 + p_2^1 z_2^4, \qquad p^3 = p_1^3\bar{z}_3^4 + p_2^3 z_4^4.$$

The parameter values of the simulations are listed in Table 18.

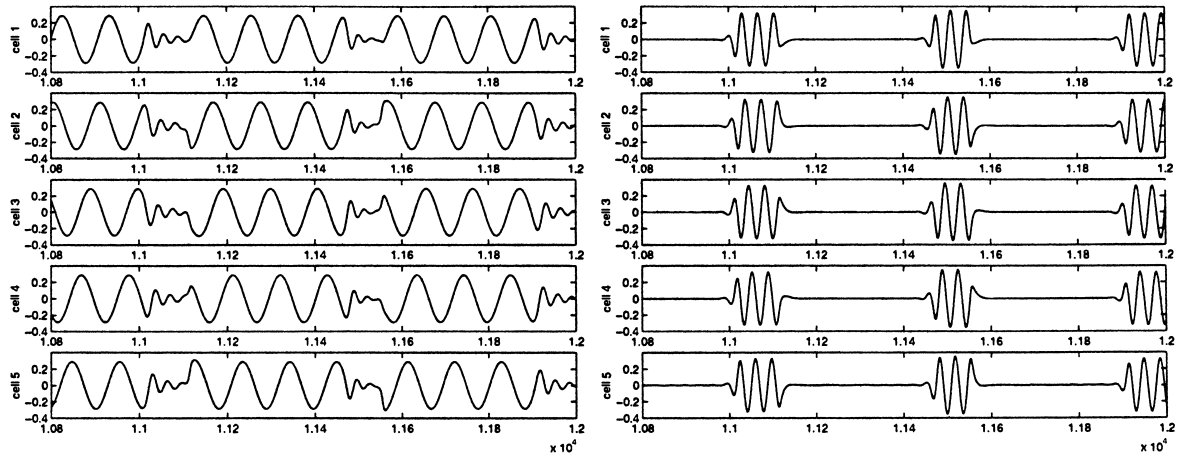

Fig. 13. Heteroclinic cycle connecting rotating waves in Hopf/Hopf mode interaction. (Left) Cycle viewed from a coordinate in the first mode. (Right) Cycle viewed from a coordinate in the second mode.

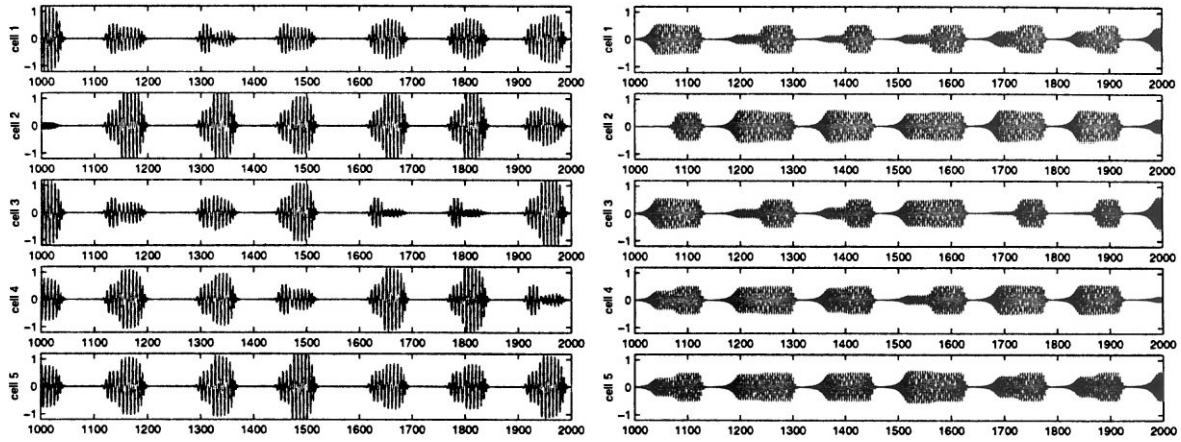

Fig. 14. Intermittency between six states in a Hopf/Hopf mode interaction: SW1, SW2, and RW in each mode. (Left) Time series from a coordinate in the first mode. (Right) Time series from a coordinate in the second mode. The trajectory approaches SW2 around 1000, 1650, 1800 and 1950 in the first mode, and around 1050, 1700, 1850, and 2000 in the second mode.

Table 18
Parameter values of the $\mathbf{D}_5 \times \mathbf{T}^2$ normal form equations and the $\mathbf{D}_5$-equivariant perturbation terms of the numerical simulations of Figs. 11,13 and 14

	SW	RW	SW–RW
$a^1_{N_1}$	−1.5	−1.5	−0.3
$a^1_{N_2}$	−2.2	0.1	−3.55
$b^1_{N_1}$	−2.0	−1.05	−1.75
$b^1_{N_2}$	−2.0	−1.2	−1.667
a^2	0.1	0.1	0.9
b^2	0.14142	0.14142	1.4
a^3	2.5	−0.3	0.625
b^3	0	1.2	0.25
a^4	0.5	0.5	0
b^4	0	0.7	0
a^5	0	−1.2	−3.45
b^5	1.5	−0.4	−0.583
a^6	0	0.9	0
b^6	−0.25	−0.25	0
a^7	2.0	0	0.125
b^7	−3.0	0	3.0
a^8	0	0	7.0
b^8	0	0	6.0
q^1_1	−0.9	0.9	0.003
q^2_1	−1.2	−0.8	0.002
r^1_1	−1.45	−1.45	0.008
r^2_1	1.15	0.95	0.004
p^1_1	5.2	0	−0.56
p^1_2	4.8	0	−0.72
p^3_1	5.3	0	−0.21
p^3_2	4.9	0	0.43

5. Remarks on cycles in n-cell rings

We now discuss the existence of heteroclinic cycles in ring systems with $\mathbf{D}_n$-symmetry. In the case of cycles connecting steady states and periodic solutions, there are similarities and differences between the cases when n is even and n is odd, as we now discuss.

Heteroclinic cycles do not exist in the $\mathbf{D}_5 \times \mathbf{S}^1$ steady-state/Hopf mode interaction normal form equations because the isotropy lattice of $\mathbf{D}_5 \times \mathbf{S}^1$ acting on $\mathbf{C}^3$ lacks the structure of Fig. 2 [3]. This lack of structure, however, does not prevent the existence of intermittent behavior in cell systems with $\mathbf{D}_5$-symmetry. In fact, we showed this intermittency in [3] using numerical integration of the general $\mathbf{D}_5 \times \mathbf{S}^1$-equivariant vector field on the six-dimensional center subspace of a steady-state/Hopf mode interaction (see Fig. 15).

The basis for this intermittency can be understood as follows. To lowest order, the $\mathbf{D}_5 \times \mathbf{S}^1$-equivariants are $\mathbf{O}(2) \times \mathbf{S}^1$-equivariant. Since cycles exist in $\mathbf{O}(2)$ mode interactions [13] (see Fig. 3), we may think of the $\mathbf{D}_5$ case as a (small) perturbation (or discretization) of the $\mathbf{O}(2)$ case. When the $\mathbf{O}(2)$ cycle is asymptotically stable, then normal hyperbolicity arguments prove the existence of intermittency in the $\mathbf{D}_5$ case, even though no heteroclinic cycle is present. In fact the situation is not too different from the $\mathbf{D}_6$ case. Here there is a heteroclinic cycle in the $\mathbf{D}_6 \times \mathbf{S}^1$ normal form — but not one when the normal form $\mathbf{S}^1$-symmetry is broken. Nevertheless, intermittency persists. These assertions have already been confirmed by the results of Section 3, where a cycle in a ring of six cells with $\mathbf{D}_6$-symmetry was studied. Specifically, recall Fig. 6 where periodic solutions appear for approximately constant lengths of time. The same conclusions follow for large values of n — depending on whether n is odd or even.

In Section 4, we sketched the proof of existence of asymptotically stable cycles in the $\mathbf{D}_n \times \mathbf{T}^2$ Hopf/Hopf mode interaction normal form equations for all $n \geq 5$. As in the steady-state/Hopf case, normal hyperbolicity guarantees that cycling behavior persists in the $\mathbf{D}_n$ ring system.

In $\mathbf{O}(2)$ Hopf/Hopf mode interactions a cycle between standing waves and rotating wave exists. This is due to the fact that amplitudes and phases decouple in the fixed-point subspaces that connect standing waves and rotating wave solutions (see [22]). In Section 4.4, we showed that a heteroclinic cycle between standing waves and rotating waves does not exist generically in the Hopf/Hopf $\mathbf{D}_n \times \mathbf{T}^2$ normal form. In [3], however, simulations of the $\mathbf{O}(2) \times \mathbf{T}^2$ normal forms with small $\mathbf{D}_5$-symmetry-breaking terms show intermittent behavior connecting two types of standing waves and rotating waves in each mode. Again, normal hyperbolicity of the asymptotically stable cycle in $\mathbf{O}(2) \times \mathbf{T}^2$ is used to find intermittent behavior in the $\mathbf{D}_5$-symmetric system. Fig. 14 is a numerical simulation showing the realization of cycling behavior of [3] in a ring of five cells.

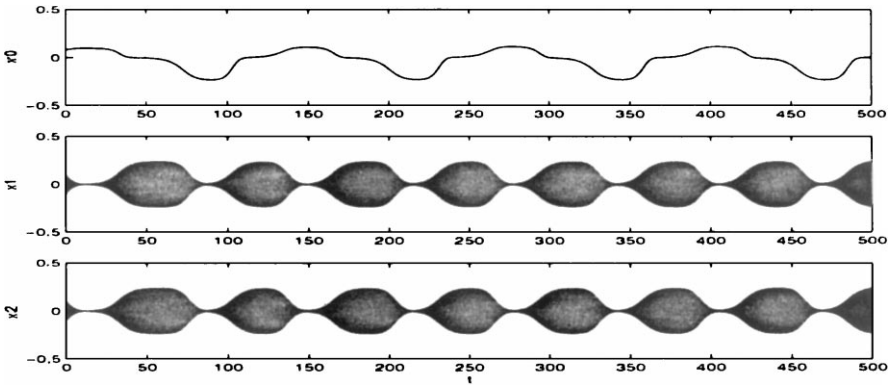

Fig. 15. Trajectory visiting intermittently a steady-state and a standing wave in a system of differential equations with $\mathbf{D}_5 \times \mathbf{S}^1$-symmetry.

Acknowledgements

We would like to thank Ian Melbourne and Mike Field for many useful discussions. This research was supported in part by an NSF Grant DMS-9704980 and the Texas Advanced Research Program (003652037). The research of PLB was supported in part by the Engineering and Physical Sciences Research Council (EPSRC:GR/L60029).

Appendix A. $\mathbf{D}_6$-invariants and-equivariants: proofs

Proof of Proposition 2.1. We derive the $\mathbf{D}_6 \times \mathbf{S}^1$-invariants by starting with the $\mathbf{S}^1$-invariants. The complex-valued $\mathbf{S}^1$-invariants are generated by

$$z_0, \qquad \bar{z}_0, \qquad u_1 = z_1\bar{z}_1, \qquad u_2 = z_2\bar{z}_2, \qquad v = z_1\bar{z}_2, \qquad \bar{v}$$

with the relation $u_1u_2 = v\bar{v}$. Letting $N = u_1 + u_2$ and $\delta = u_2 - u_1$, we find an alternate basis

$$z_0, \qquad \bar{z}_0, \qquad N, \qquad \delta, \qquad v, \qquad \bar{v}$$

with the relation $4v\bar{v} = N^2 - \delta^2$. In this basis the $\mathbf{S}^1$-invariant can be written uniquely as

$$\sum a_{\alpha\beta} z_0^\alpha v^\beta + b_{\alpha\beta}\bar{z}_0^\alpha v^\beta + c_{\alpha\beta} z_0^\alpha \bar{v}^\beta + d_{\alpha\beta}\bar{z}_0^\alpha \bar{v}^\beta,$$

where $a_{\alpha\beta}$, $b_{\alpha\beta}$, $c_{\alpha\beta}$, $d_{\alpha\beta}$ are complex-valued functions of ρ, N, and δ. The reality of these invariants implies that $d_{\alpha\beta} = \bar{a}_{\alpha\beta}$ and $c_{\alpha\beta} = \bar{b}_{\alpha\beta}$. Therefore, the general real-valued $\mathbf{S}^1$-invariant is

$$\sum a_{\alpha\beta} z_0^\alpha v^\beta + \bar{a}_{\alpha\beta}\bar{z}_0^\alpha \bar{v}^\beta + b_{\alpha\beta}\bar{z}_0^\alpha v^\beta + \bar{b}_{\alpha\beta} z_0^\alpha \bar{v}^\beta.$$

Next, the $\mathbf{Z}_6 \subset \mathbf{D}_6$-action on (z_0, N, δ, v) is generated by

$$\gamma(z_0, N, \delta, v) = (\mathrm{e}^{\gamma \mathrm{i}} z_0, N, \delta, \mathrm{e}^{2\gamma \mathrm{i}} v).$$

This action leaves ρ, N, and δ invariant. It also implies that $a_{\alpha\beta} = b_{\alpha\beta} = 0$ unless

$$\alpha + 2\beta = 0 \bmod 6, \qquad -\alpha + 2\beta = 0 \bmod 6.$$

These cases lead to generators $z_0^{6l-2\beta} v^\beta$ ($3l \geq \beta \geq 0$) and $\bar{z}_0^{6l+2\beta} v^\beta$ ($\beta \geq 0, \beta \geq -3l$) plus their complex conjugates.

We now find a minimal set of generators. Using the identities

$$\begin{aligned} z_0^{6l-2\beta} v^\beta &= (v^3 + \bar{v}^3) z_0^{6(l-1)-2(\beta-3)} v^{\beta-3} - (v\bar{v})^3 z_0^{6(l-2)-2(\beta-6)} v^{\beta-6}, \\ \bar{z}_0^{6l+2\beta} v^\beta &= (v^3 + \bar{v}^3) \bar{z}_0^{6(l+1)+2(\beta-3)} v^{\beta-3} - (v\bar{v})^3 \bar{z}_0^{6(l+2)+2(\beta-6)} v^{\beta-6}, \end{aligned}$$

the fact that $v^3 + \bar{v}^3$ and $v\bar{v}$ are invariant functions, and the induction on β, we see that $\beta \geq 6$ yield redundant generators. Observe that

$$\begin{aligned} z_0^{6l-10} v^5 &= (v^3 + \bar{v}^3) z_0^{6(l-1)-4} v^2 - (v\bar{v})^2 z_0^{6(l-2)+2} \bar{v}, \\ z_0^{6l-8} v^4 &= (v^3 + \bar{v}^3) z_0^{6(l-1)-2} v - (v\bar{v}) z_0^{6(l-2)+4} \bar{v}^2, \\ \bar{z}_0^{6l+10} v^5 &= (v^3 + \bar{v}^3) \bar{z}_0^{6(l+1)+4} v^2 - (v\bar{v})^2 \bar{z}_0^{6(l+2)-2} \bar{v}, \\ \bar{z}_0^{6l+8} v^4 &= (v^3 + \bar{v}^3) \bar{z}_0^{6(l+1)+2} v - (v\bar{v}) \bar{z}_0^{6(l+2)-4} \bar{v}^2. \end{aligned}$$

Therefore, we can reduce the set of generators to $0 \leq \beta \leq 3$.

Similarly, we use the identities

$$z_0^{6l-2\beta}v^\beta = (z_0^6+\bar z_0^6)z_0^{6(l-1)-2\beta}v^\beta - (z_0\bar z_0)^6 z_0^{6(l-2)-2\beta}v^\beta,$$
$$z_0^{12-2\beta}v^\beta = (z_0^6+\bar z_0^6)z_0^{6-2\beta}v^\beta - (z_0\bar z_0)^{6-2\beta}\bar z_0^{2\beta}v^\beta,$$
$$\bar z_0^{6l+2\beta}v^\beta = (z_0^6+\bar z_0^6)\bar z_0^{6(l-1)+2\beta}v^\beta - (z_0\bar z_0)^6\bar z_0^{6(l-2)+2\beta}v^\beta$$

to arrive at a set of generators with $l \le 1$. Possible generators of the form $z_0^{6l-2\beta}v^\beta$ are $C = v^3$, $D = z_0^2v^2$, $E = z_0^4v$, and $B = z_0^6$. When $l = 1$, we have the following identity for generators of the form $\bar z_0^{6l+2\beta}v^\beta$:

$$\bar z_0^{6+2\beta}v^\beta = (z_0^6+\bar z_0^6)\bar z_0^{2\beta}v^\beta - (z_0\bar z_0)^{2\beta}z_0^{6-2\beta}v^\beta.$$

Thus, we can assume that $l = 0$ and we have possible generators $\bar A = \bar z_0^2 v$, $\bar z_0^4 v^2$, and $\bar z_0^6 v^3$. Since

$$\bar z_0^4 v^2 = \bar A^2, \qquad \bar z_0^6 v^3 = (z_0^6+\bar z_0^6)C - DE,$$

we have shown that $\{A, \dots, E\}$ is a set of $\mathbf{Z}_6 \times \mathbf{S}^1$ generators.

Finally, we can decompose each $a_{\alpha\beta}$ and $b_{\alpha\beta}$ into an even and an odd function in δ, obtaining

$$a_{\alpha\beta} = A^1_{\alpha\beta}(\rho, N, \Delta) + A^2_{\alpha\beta}(\rho, N, \Delta)\delta, \qquad b_{\alpha\beta} = B^1_{\alpha\beta}(\rho, N, \Delta) + B^2_{\alpha\beta}(\rho, N, \Delta)\delta,$$

where $A^j_{\alpha\beta}$ and $B^j_{\alpha\beta}$ are complex-valued $\mathbf{D}_6 \times \mathbf{S}^1$-invariant functions. Thus, we can write the general real-valued $\mathbf{S}^1$-invariant function as

$$\sum (A^1_{\alpha\beta} + \delta A^2_{\alpha\beta})z_0^\alpha v^\beta + (\bar A^1_{\alpha\beta} + \delta \bar A^2_{\alpha\beta})\bar z_0^\alpha \bar v^\beta + (B^1_{\alpha\beta} + \delta B^2_{\alpha\beta})\bar z_0^\alpha v^\beta + (\bar B^1_{\alpha\beta} + \delta \bar B^2_{\alpha\beta})z_0^\alpha \bar v^\beta.$$

Now observe that the action of $\kappa \in \mathbf{D}_6$ on (z_0, N, δ, v) is

$$\kappa(z_0, N, \delta, v) = (\bar z_0, N, -\delta, \bar v),$$

which implies that $A^1_{\alpha\beta}$, $B^1_{\alpha\beta} \in \mathbf{R}$ and $A^2_{\alpha\beta}$, $B^2_{\alpha\beta} \in \mathbf{R}\{i\}$. Thus, redefining $A^2_{\alpha\beta}$, $B^2_{\alpha\beta} \in \mathbf{R}$, we can write the general invariant function as

$$\sum A^1_{\alpha\beta}(z_0^\alpha v^\beta + \bar z_0^\alpha \bar v^\beta) + A^2_{\alpha\beta}\mathrm{i}\delta(z_0^\alpha v^\beta - \bar z_0^\alpha \bar v^\beta) + B^1_{\alpha\beta}(\bar z_0^\alpha v^\beta + z_0^\alpha \bar v^\beta) + B^2_{\alpha\beta}\mathrm{i}\delta(\bar z_0^\alpha v^\beta - z_0^\alpha \bar v^\beta). \tag{A.1}$$

Substitution in (A.1) of the minimal set of $\mathbf{Z}_6 \times \mathbf{S}^1$ generators computed above yields a complete set of generators for the $\mathbf{D}_6 \times \mathbf{S}^1$-invariants. □

Proof of Proposition 2.2. Let $g(z) = (g_0, g_1, g_2)$ be a $\mathbf{D}_6 \times \mathbf{S}^1$-equivariant mapping $\mathbf{C}^3 \mapsto \mathbf{C}^3$. Commutativity of g with $\mathbf{S}^1$ implies that we can write g in the form

$$g = (a, bz_1 + cz_2, dz_1 + ez_2),$$

where a, b, c, and d are complex-valued $\mathbf{S}^1$-invariant functions of z_0, N, δ, and v. Commutativity with κ additionally requires that

$$a(z) = \bar a(\kappa z), \tag{A.2}$$

$$b(z)z_1 + c(z)z_2 = e(\kappa z)z_1 + d(\kappa z)z_2, \tag{A.3}$$

where $z = (z_0, N, \delta, v)$ and $\kappa z = (\bar{z}_0, N, -\delta, \bar{v})$. Using the relations $vz_2 = \frac{1}{2}(N+\delta)z_1$ and $\bar{v}z_1 = \frac{1}{2}(N-\delta)z_2$, we can write the coefficients in (A.3) as functions of the form

$$b = b(z_0, v, N, \delta), \qquad c = c(z_0, \bar{v}, N, \delta), \qquad d = d(z_0, \bar{v}, N, \delta), \qquad e = e(z_0, v, N, \delta). \tag{A.4}$$

This shows that $b(z) - e(\kappa z)$ and $c(z) - d(\kappa z)$ are linearly independent so that $d(z) = c(\kappa z)$ and $e(z) = b(\kappa z)$. Then g takes the form

$$g = (a(z), b(z)z_1 + c(z)z_2, c(\kappa z)z_1 + b(\kappa z)z_2).$$

Now commutativity of g with γ imposes the following conditions:

$$a(z) = \mathrm{e}^{-\gamma \mathrm{i}} a(\gamma z), \qquad b(z)z_1 + c(z)z_2 = b(\gamma z)z_1 + \mathrm{e}^{-2\gamma \mathrm{i}} c(\gamma z)z_2.$$

Let $R(z) = (b(z) - b(\gamma z))z_1$ and $S(z) = (c(z) - \mathrm{e}^{-2\gamma \mathrm{i}} c(\gamma z))z_2$. Again we need to show that R and S are linearly independent, thus verifying that $b(z) = b(\gamma z)$ and $c(z) = \mathrm{e}^{-2\gamma \mathrm{i}} c(\gamma z)$. We do this as follows. Using (A.4), we write R and S as polynomials of the form $R(z) = r(z_0, v, N, \delta)z_1$ and $S(z) = s(z_0, \bar{v}, N, \delta)z_2$. Typical terms in their Taylor expansion are $z_0^{\tilde{m}} v^{\tilde{n}} N^{\tilde{k}} \delta^{\tilde{l}} z_1$ and $z_0^m \bar{v}^n N^k \delta^l z_2$, respectively, where $m, n, k, l, \tilde{m}, \tilde{n}, \tilde{k}, \tilde{l}$ are all nonnegative integers. Term by term comparison yields $\tilde{n} = -(n+1)$ which is a contradiction to $\tilde{n}$ being a nonnegative integer. Thus, R and S are linearly independent. Summarizing, commutativity with γ requires

$$a = \mathrm{e}^{-\gamma \mathrm{i}} a(\gamma z), \tag{A.5}$$

$$b = b(\gamma z), \tag{A.6}$$

$$c = \mathrm{e}^{-2\gamma \mathrm{i}} c(\gamma z). \tag{A.7}$$

Next we calculate the generators for a. As in the derivation of the $\mathbf{D}_6 \times \mathbf{S}^1$-invariants, we can write

$$a(z_0, N, \delta, v) = \sum a_{\alpha\beta} z_0^\alpha v^\beta + b_{\alpha\beta} \bar{z}_0^\alpha v^\beta + c_{\alpha\beta} z_0^\alpha \bar{v}^\beta + d_{\alpha\beta} \bar{z}_0^\alpha \bar{v}^\beta,$$

where $a_{\alpha\beta}$, $b_{\alpha\beta}$, $c_{\alpha\beta}$, and $d_{\alpha\beta}$ are complex-valued $\mathbf{D}_6 \times \mathbf{S}^1$-invariant functions of ρ, N, and δ. The commutativity condition (A.2) implies $a_{\alpha\beta} = b_{\alpha\beta} = c_{\alpha\beta} = c_{\alpha\beta} = d_{\alpha\beta} = 0$, unless

$$\alpha + 2\beta - 1 = 0 \bmod 6, \qquad \alpha - 2\beta - 1 = 0 \bmod 6,$$
$$-\alpha + 2\beta - 1 = 0 \bmod 6, \qquad -\alpha - 2\beta - 1 = 0 \bmod 6.$$

These cases lead to generators $z_0^{6l-2\beta+1} v^\beta$ $(3l \geq \beta \geq 0)$, $\bar{z}_0^{6l+2\beta-1} v^\beta$ $(\beta \geq 0, \beta \geq -3l+1)$, $z_0^{6l+2\beta+1} \bar{v}^\beta$ $(\beta \geq 0, \beta \geq -3l)$, and $\bar{z}_0^{6l-2\beta-1} \bar{v}^\beta$ $(3l-1 \geq \beta \geq 0)$.

We now find a minimal set of generators. Using the identities

$$z_0^{6l-2\beta+1} v^\beta = (v^3 + \bar{v}^3) z_0^{6(l-1)-2(\beta-3)+1} v^{\beta-3} - (v\bar{v})^3 z_0^{6(l-2)-2(\beta-6)+1} v^{\beta-6},$$

$$\bar{z}_0^{6l+2\beta-1} v^\beta = (v^3 + \bar{v}^3) \bar{z}_0^{6(l+1)+2(\beta-3)+1} v^{\beta-3} - (v\bar{v})^3 \bar{z}_0^{6(l+2)+2(\beta-6)+1} v^{\beta-6},$$

$$z_0^{6l+2\beta+1} \bar{v}^\beta = (v^3 + \bar{v}^3) z_0^{6(l+1)+2(\beta-3)+1} \bar{v}^{\beta-3} - (v\bar{v})^3 z_0^{6(l+2)+2(\beta-6)+1} \bar{v}^{\beta-6},$$

$$\bar{z}_0^{6l-2\beta-1} \bar{v}^\beta = (v^3 + \bar{v}^3) \bar{z}_0^{6(l-1)-2(\beta-3)-1} \bar{v}^{\beta-3} - (v\bar{v})^3 z_0^{6(l-2)-2(\beta-6)-1} \bar{v}^{\beta-6},$$

the fact that $v^3 + \bar{v}^3$ and $v\bar{v}$ are invariant functions, and induction on β, we see that $\beta \geq 6$ yields redundant

generators. Observe that

$$
\begin{aligned}
z_0^{6l-9}v^5 &= (v^3+\bar v^3)z_0^{6(l-1)-3}v^2 - (v\bar v)^2 z_0^{6(l-2)+3}\bar v,\\
z_0^{6l-7}v^4 &= (v^3+\bar v^3)z_0^{6(l-1)-1}v - (v\bar v)z_0^{6(l-2)+5}\bar v^2,\\
\bar z_0^{6l+9}v^5 &= (v^3+\bar v^3)\bar z_0^{6(l+1)+3}v^2 - (v\bar v)^2 \bar z_0^{6(l+2)-3}\bar v,\\
\bar z_0^{6l+7}v^4 &= (v^3+\bar v^3)\bar z_0^{6(l+1)+1}v - (v\bar v)\bar z_0^{6(l+2)-5}\bar v^2,\\
z_0^{6l+11}v^5 &= (v^3+\bar v^3)z_0^{6(l+1)+5}\bar v^2 - (v\bar v)^2 z_0^{6(l+2)-1}v,\\
z_0^{6l+9}v^4 &= (v^3+\bar v^3)z_0^{6(l+1)+3}\bar v - (v\bar v)z_0^{6(l+2)-3}v^2,\\
\bar z_0^{6l-11}v^5 &= (v^3+\bar v^3)\bar z_0^{6(l-1)-5}\bar v^2 - (v\bar v)^2 \bar z_0^{6(l-2)+1}v,\\
\bar z_0^{6l-9}v^4 &= (v^3+\bar v^3)\bar z_0^{6(l-1)-3}v - (v\bar v)\bar z_0^{6(l-2)+3}v^2.
\end{aligned}
$$

Therefore, we can reduce the set of generators to $0 \le \beta \le 3$.

Similarly, we use the identities

$$
\begin{aligned}
z_0^{6l-2\beta+1}v^\beta &= (z_0^6+\bar z_0^6)z_0^{6(l-1)-2\beta+1}v^\beta - (z_0\bar z_0)^6 z_0^{6(l-2)-2\beta+1}v^\beta,\\
z_0^{12-2\beta+1}v^\beta &= (z_0^6+\bar z_0^6)z_0^{6-2\beta+1}v^\beta - (z_0\bar z_0)^{6-2\beta+1}\bar z_0^{2\beta-1}v^\beta,\\
\bar z_0^{6l+2\beta-1}v^\beta &= (z_0^6+\bar z_0^6)\bar z_0^{6(l-1)+2\beta-1}v^\beta - (z_0\bar z_0)^6 \bar z_0^{6(l-2)+2\beta-1}v^\beta,\\
\bar z_0^{6l-2\beta-1}\bar v^\beta &= (z_0^6+\bar z_0^6)\bar z_0^{6(l-1)-2\beta-1}\bar v^\beta - (z_0\bar z_0)^6 z_0^{6(l-2)-2\beta-1}\bar v^\beta,\\
\bar z_0^{12-2\beta-1}\bar v^\beta &= (z_0^6+\bar z_0^6)\bar z_0^{6-2\beta-1}\bar v^\beta - (z_0\bar z_0)^{6-2\beta-1} z_0^{2\beta+1}\bar v^\beta,\\
z_0^{6l+2\beta+1}\bar v^\beta &= (z_0^6+\bar z_0^6)z_0^{6(l-1)+2\beta+1}\bar v^\beta - (z_0\bar z_0)^6 z_0^{6(l-2)+2\beta+1}\bar v^\beta
\end{aligned}
$$

to arrive at a set of generators with $l \le 1$. Possible generators for $z_0^{6l-2\beta+1}v^\beta$ and $\bar z_0^{6l-2\beta-1}\bar v^\beta$ are as follows:

$$
z_0^{6l-2\beta+1}v^\beta: \quad z_0v^3,\ z_0^3v^2,\ z_0^5v,\ z_0,\ z_0^7, \qquad \bar z_0^{6l-2\beta-1}\bar v^\beta: \quad \bar z_0\bar v^2,\ \bar z_0^3\bar v,\ \bar z_0^5.
$$

When $l = 1$, we have the following identity for generators of the form $\bar z_0^{6l+2\beta-1}v^\beta$ and $z_0^{6l+2\beta+1}\bar v^\beta$:

$$
\begin{aligned}
\bar z_0^{6+2\beta-1}v^\beta &= (z_0^6+\bar z_0^6)\bar z_0^{2\beta-1}v^\beta - (z_0\bar z_0)^{2\beta-1}z_0^{6-2\beta+1}v^\beta,\\
z_0^{6+2\beta+1}\bar v^\beta &= (z_0^6+\bar z_0^6)z_0^{2\beta+1}\bar v^\beta - (z_0\bar z_0)^{2\beta+1}\bar z_0^{6-2\beta-1}\bar v^\beta.
\end{aligned}
$$

Thus, we can assume that $l = 0$ and we have possible generators

$$
\bar z_0^{6l+2\beta-1}v^\beta: \quad \bar z_0v,\ \bar z_0^3v^2,\ \bar z_0^5v^3, \qquad \bar z_0^{6l-2\beta-1}\bar v^\beta: \quad z_0,\ z_0^3\bar v,\ z_0^5\bar v^2,\ z_0^7\bar v^3.
$$

Since

$$
\begin{aligned}
&z_0^3v^2 = (z_0^2v^2+\bar z_0^2\bar v^2)z_0 - (z_0\bar z_0)\bar z_0\bar v^2, \qquad \bar z_0^5v^3 = (z_0^2\bar v+\bar z_0^2v)\bar z_0^3v^2 - (z_0\bar z_0)(v\bar v)\bar z_0v,\\
&z_0^5v = (z_0^4v+\bar z_0^4\bar v)z_0 - (z_0\bar z_0)\bar z_0^3\bar v, \qquad z_0^3\bar v = (z_0^2\bar v+\bar z_0^2v)z_0 - (z_0\bar z_0)\bar z_0v, \qquad z_0^7 = (z_0)^7,\\
&z_0^5\bar v^2 = (z_0^2\bar v+\bar z_0^2v)z_0^3\bar v - (z_0\bar z_0)^2(v\bar v)z_0, \qquad \bar z_0^3v^2 = (z_0^2\bar v+\bar z_0^2v)\bar z_0v - (z_0\bar z_0)(v\bar v)z_0,\\
&z_0^7\bar v^3 = (z_0^2\bar v+\bar z_0^2v)z_0^5\bar v^2 - (z_0\bar z_0)^2(v\bar v)z_0^3\bar v,
\end{aligned}
$$

we have shown that $\{z_0, \bar z_0z_1\bar z_2, \bar z_0^5, \bar z_0\bar v^2, \bar z_0^3\bar v, z_0v^3\}$ is a set of $\mathbf{Z}_6 \times \mathbf{S}^1$-equivariant generators for a.

Finally, we can decompose each $a_{\alpha\beta}$, $b_{\alpha\beta}$, $c_{\alpha\beta}$, and $d_{\alpha\beta}$ into an even and an odd function in δ, obtaining

$$
\begin{aligned}
a_{\alpha\beta} &= A^1_{\alpha\beta}(\rho, N, \Delta) + A^2_{\alpha\beta}(\rho, N, \Delta)\delta, \qquad b_{\alpha\beta} = B^1_{\alpha\beta}(\rho, N, \Delta) + B^2_{\alpha\beta}(\rho, N, \Delta)\delta,\\
c_{\alpha\beta} &= C^1_{\alpha\beta}(\rho, N, \Delta) + C^2_{\alpha\beta}(\rho, N, \Delta)\delta, \qquad d_{\alpha\beta} = D^1_{\alpha\beta}(\rho, N, \Delta) + D^2_{\alpha\beta}(\rho, N, \Delta)\delta,
\end{aligned}
$$

where $A^j_{\alpha\beta}$, $B^j_{\alpha\beta}$, $C^j_{\alpha\beta}$, and $D^j_{\alpha\beta}$ are complex-valued $\mathbf{D}_6 \times \mathbf{S}^1$-invariant functions. Thus, we can write a as

$$a(z_0, N, \delta, v) = \sum (A^1_{\alpha\beta} + \delta A^2_{\alpha\beta}) z_0^\alpha v^\beta + (B^1_{\alpha\beta} + \delta B^2_{\alpha\beta}) \bar{z}_0^\alpha v^\beta + \sum (C^1_{\alpha\beta} + \delta C^2_{\alpha\beta}) z_0^\alpha \bar{v}^\beta + (D^1_{\alpha\beta} + \delta D^2_{\alpha\beta}) \bar{z}_0^\alpha \bar{v}^\beta.$$

Now observe that the action of $\kappa \in \mathbf{D}_6$ on (z_0, N, δ, v) is

$$\kappa(z_0, N, \delta, v) = (\bar{z}_0, N, -\delta, \bar{v}),$$

which implies that $A^1_{\alpha\beta}$, $B^1_{\alpha\beta}$, $C^1_{\alpha\beta}$, and $D^1_{\alpha\beta} \in \mathbf{R}$ and $A^2_{\alpha\beta}$, $B^2_{\alpha\beta}$, $C^2_{\alpha\beta}$, and $B^2_{\alpha\beta} \in \mathbf{R}\{i\}$. Thus, redefining $A^2_{\alpha\beta}$, $B^2_{\alpha\beta}$, $C^2_{\alpha\beta}$, and $D^2_{\alpha\beta} \in \mathbf{R}$, we can write

$$a(z_0, N, \delta, v) = \sum (A^1_{\alpha\beta} + \mathrm{i}\delta A^2_{\alpha\beta}) z_0^\alpha v^\beta + (B^1_{\alpha\beta} + \mathrm{i}\delta B^2_{\alpha\beta}) \bar{z}_0^\alpha v^\beta + \sum (C^1_{\alpha\beta} + \mathrm{i}\delta C^2_{\alpha\beta}) z_0^\alpha \bar{v}^\beta + (D^1_{\alpha\beta} + \mathrm{i}\delta D^2_{\alpha\beta}) \bar{z}_0^\alpha \bar{v}^\beta. \tag{A.8}$$

Substitution in (A.8) of the minimal set of $\mathbf{Z}_6 \times \mathbf{S}^1$ generators for a yields, modulo the $\mathbf{D}_6 \times \mathbf{S}^1$-invariants, a complete set of $\mathbf{D}_6 \times \mathbf{S}^1$-equivariant generators for $g_0 : V^1, \ldots, V^6$ and $\mathrm{i}\delta V^1, \ldots, \mathrm{i}\delta V^6$.

Next we consider g_1 and g_2. Recall that b is a $\mathbf{Z}_6 \times \mathbf{S}^1$-invariant function. Its generators are the $\mathbf{D}_6 \times \mathbf{S}^1$-invariants over the complex numbers. Decompose b into an even and an odd function in the δ coordinate: $b = b^0 + b^1$. Then g_1 takes the form

$$g_1 = (P + Q\delta) z_1,$$

where P and Q are complex-valued $\mathbf{D}_6 \times \mathbf{S}^1$-invariant functions. The equivariance condition $c(\kappa z) = b(z)$, specifies g_2 in terms of g_1,

$$g_2 = (P - Q\delta) z_2.$$

Letting $P = p + q\mathrm{i}$ and $Q = r + s\mathrm{i}$, we find generators V^7, $\mathrm{i}V^7$, δV^8, and $\mathrm{i}\delta V^8$.

We now compute the generators for c. Write

$$c(z_0, N, \delta, v) = \sum a_{\alpha\beta} z_0^\alpha v^\beta + b_{\alpha\beta} \bar{z}_0^\alpha v^\beta + c_{\alpha\beta} z_0^\alpha \bar{v}^\beta + d_{\alpha\beta} \bar{z}_0^\alpha \bar{v}^\beta,$$

where $a_{\alpha\beta}$, $b_{\alpha\beta}$, $c_{\alpha\beta}$, and $d_{\alpha\beta}$ are complex-valued $\mathbf{D}_6 \times \mathbf{S}^1$-invariant functions of ρ, N, and δ. The commutativity condition (A.7) implies that $a_{\alpha\beta} = b_{\alpha\beta} = c_{\alpha\beta} = d_{\alpha\beta} = 0$, unless

$$\alpha + 2\beta - 2 = 0 \bmod 6, \qquad \alpha - 2\beta - 2 = 0 \bmod 6,$$
$$-\alpha + 2\beta - 2 = 0 \bmod 6, \quad -\alpha - 2\beta - 2 = 0 \bmod 6.$$

A similar set of calculations yields, modulo the $\mathbf{D}_6 \times \mathbf{S}^1$-invariants, the remaining equivariant maps $V^9, \ldots, \mathrm{i}\delta V^{16}$. □

References

[1] D. Armbruster, J. Guckenheimer, P. Holmes, Heteroclinic cycles and modulated travelling waves in systems with $\mathbf{O}(2)$-symmetry, Physica D 29 (1988) 257–282.

[2] D.G. Aronson, M. Golubitsky, M. Krupa, Coupled arrays of Josephson junctions and bifurcation of maps with S_N-symmetry, Nonlinearity 4 (1991) 861–902.

[3] P.-L. Buono, M. Golubitsky, A. Palacios, Heteroclinic cycles in systems with $\mathbf{D}_n$-symmetry, in: Z. Chen, S.-N. Chow, K. Li (Eds.), Bifurcation Theory and its Numerical Analysis, Springer, Singapore, 1999, pp. 13–27.
[4] J.J. Collins, I. Stewart, Coupled nonlinear oscillators and the symmetries of animal gaits, J. Nonlinear Sci. 3 (1993) 349–392.
[5] J.J. Collins, I. Stewart, Hexapodal gaits and coupled nonlinear oscillator models, Biol. Cybernet. 68 (1993) 287–298.
[6] J.J. Collins, I. Stewart, A group-theoretic approach to rings of coupled biological oscillators, Biol. Cybernet. 71 (1994) 95–103.
[7] B. Dionne, M. Golubitsky, I. Stewart, Coupled cells with internal symmetry. I. Wreath products, Nonlinearity 9 (1996) 559–574.
[8] B. Dionne, M. Golubitsky, I. Stewart, Coupled cells with internal symmetry. II. Direct products, Nonlinearity 9 (1996) 575–599.
[9] M.J. Field, Equivariant dynamical systems, Trans. Am. Math. Soc. 259 (1) (1980) 185–205.
[10] M.J. Field, Lectures on Bifurcations, Dynamics and Symmetry, Pitman Research Notes, Vol. 356, Addison-Wesley, Harlow, 1996.
[11] M. Golubitsky, I. Stewart, Symmetry and pattern formation in coupled cell networks, in: M. Golubitsky, D. Luss, S.H. Strogatz (Eds.), Pattern Formation in Continuous and Coupled Systems, IMA Volumes in Mathematics and its Applications, Vol. 115, Springer, New York, 1999, pp. 65–82.
[12] M. Golubitsky, I. Stewart, P.-L. Buono, J.J. Collins, A modular network for legged locomotion, Physica D 115 (1998) 56–72.
[13] M. Golubitsky, I. Stewart, D.G. Schaeffer, Singularities and Groups in Bifurcation Theory, Vol. II, Applied Mathematical Sciences, Vol. 69, Springer, New York, 1988.
[14] J. Guckenheimer, P. Holmes, Structurally stable heteroclinic cycles, Math. Proc. Cambridge Philos. Soc. 103 (1988) 189–192 .
[15] P. Hadley, M.R. Beasley, K. Wiesenfeld, Phase locking of Josephson junction series arrays, Phys. Rev. B 38 (1988) 8712–8719.
[16] N. Kopell, G.B. Ermentrout, Coupled oscillators and the design of central pattern generators, Math. Biosci. 89 (1988) 14–23.
[17] N. Kopell, G.B. Ermentrout, Phase transitions and other phenomena in chains of oscillators, SIAM J. Appl. Math. 50 (1990) 1014–1052.
[18] M. Krupa, Robust heteroclinic cycles, J. Nonlinear Sci. 7 (2) (1997) 129–176.
[19] M. Krupa, I. Melbourne, Asymptotic stability of heteroclinic cycles in systems with symmetry, Ergodic Theory Dyn. Syst. 15 (1995) 121–147.
[20] J.S.W. Lamb, I. Melbourne, Bifurcation from discrete rotating waves, Arch. Rational Mech. Anal. 149 (1999) 229–270.
[21] I. Melbourne, Intermittency as a codimension three phenomenon, Dyn. Differential Equations 1 (1989) 347–367.
[22] I. Melbourne, P. Chossat, M. Golubitsky, Heteroclinic cycles involving periodic solutions in mode interactions with $\mathbf{O}(2)$-symmetry, Proc. Roy. Soc. Edinburgh A 113 (1989) 315–345.
[23] R.H. Rand, A.H. Cohen, P.J. Holmes, Systems of coupled oscillators as models of central pattern generators, in: A.H. Cohen, S. Rossignol, S. Grillner (Eds.), Neural Control of Rhythmic Movements in Vertebrates, Wiley, New York, 1988, pp. 333–367.
[24] S. Wiggins, Introduction to Applied Nonlinear Dynamical Systems and Chaos, Applied Mathematical Sciences, Vol. 2, Springer, New York, 1990.